Precambrian Research 167 (2008) 186–200

Contents lists available at ScienceDirect

Precambrian Research

journal homepage: www.elsevier.com/locate/precamres

Detrital zircon fingerprint of the Proto-Andes: Evidence for a Neoproterozoic active margin?

David M. Chew[a,*], Tomas Magna[b], Christopher L. Kirkland[c,1], Aleksandar Mišković[d], Agustín Cardona[e], Richard Spikings[d], Urs Schaltegger[d]

[a] Department of Geology, Trinity College Dublin, Dublin 2, Ireland
[b] Institute of Mineralogy and Geochemistry, University of Lausanne, CH-1015 Lausanne, Switzerland
[c] Laboratory for Isotope Geology, Swedish Museum of Natural History, S-104 05 Stockholm, Sweden
[d] Department of Earth Sciences, University of Geneva, Rue des Maraîchers 13, 1205 Geneva, Switzerland
[e] Smithsonian Tropical Research Institute, Apartado Postal 0843-03092, Balboa, Ancon, Panama City, Panama

ARTICLE INFO

Article history:
Received 23 June 2008
Received in revised form 25 July 2008
Accepted 2 August 2008

Keywords:
Proto-Andes
Neoproterozoic
Zircon
Provenance
Iapetus

ABSTRACT

Neoproterozoic Palaeogeographic reconstructions of Rodinia conventionally place the western (Proto-Andean) margin of Amazonia against the eastern (Appalachian) margin of Laurentia. Separation and formation of the Iapetus Ocean is generally considered to have occurred later at ~550 Ma. We examine the U–Pb detrital zircon "fingerprint" of autochthonous rocks from the northern and central segments of the Proto-Andean margin, which formed part of the western margin of Amazonia during the Late Neoproterozoic–Phanerozoic. The Proto-Andean margin is clearly the most feasible source region for most of the zircon grains, except for a 550–650 Ma sub-population, broadly age-equivalent to the Brasiliano/Pan-African Orogeny in eastern Amazonia. No obvious source for this detritus is known in the northern and central Andes. Derivation from eastern Amazonia is considered unlikely due to the stark paucity of detritus derived from the core of the Amazonian craton. Instead, we propose that a Late Neoproterozoic magmatic belt is buried beneath the present-day Andean belt or Amazon Basin, and was probably covered during the Eocene–Oligocene. If this inferred Neoproterozoic belt was an active margin, it would record the initiation of Proto-Andean subduction and imply at least partial separation of West Gondwana from its conjugate rift margin of eastern Laurentia prior to ca. 650 Ma. This separation may be linked to the ca. 770–680 Ma A-type magmatism found on eastern Laurentia in the southern Appalachians, and on the Proto-Andean margin in the Sierra Pampeanas and the Eastern Cordillera of Peru.

1. Introduction

Palaeogeographic reconstructions of the Early Neoproterozoic supercontinent of Rodinia (e.g. Hoffman, 1991; Torsvik, 2003; Li et al., 2008) usually place western Amazonia against eastern Laurentia and Baltica (Fig. 1). This reconstruction is based on both geological evidence (e.g. Hoffman, 1991), isotopic data (Tohver et al., 2004) and palaeomagnetic reconstructions (e.g. Weil et al., 1998; Tohver et al., 2002; D'Agrella-Filho et al., 2008). Geological evidence includes correlation of Precambrian orogenic belts that were once continuous but are now truncated at the modern-day continental margins (Sadowski and Bettencourt, 1996; Tohver et al., 2004). The eastern Laurentia–western Amazonia link of Hoffman (1991) is based on the presence of Grenvillian belts in both eastern Laurentia and in southwest Amazonia (the Rondonia-Sunsas Belt, Figs. 1 and 2).

There is abundant evidence that the final rifting event to affect Laurentia took place during the late Neoproterozoic. Such evidence includes the stratigraphic rift-to-drift transition in Laurentian margin sequences at the Precambrian–Cambrian boundary (e.g. Bond et al., 1984; Williams and Hiscott, 1987), and the voluminous rift-related magmatism which lasted from ~620 Ma to 550 Ma (e.g. Kamo et al., 1989; Bingen et al., 1998; Cawood et al., 2001; Kinny et al., 2003). Cawood et al. (2001) invoked a multistage rift history that involved an initial separation of Laurentia from the west Gondwana cratons at ca. 570 Ma, followed by rifting of a further block or blocks from Laurentia at ca. 540–535 Ma into an already open Iapetus Ocean to establish the main passive-margin sequence in eastern Laurentia.

In contrast, the early history of the western Gondwanan margin is poorly understood compared to its conjugate margin of eastern Laurentia. This is partly a function of the limited exposure

* Corresponding author. Tel.: +353 1 8963481; fax: +353 1 6711199.
E-mail address: chewd@tcd.ie (D.M. Chew).
[1] Present address: Geological Survey, Resources Group, Department of Industry and Resources, 100 Plain Street, East Perth, Western Australia 6004, Australia.

0301-9268/$ – see front matter © 2008 Elsevier B.V. All rights reserved.
doi:10.1016/j.precamres.2008.08.002

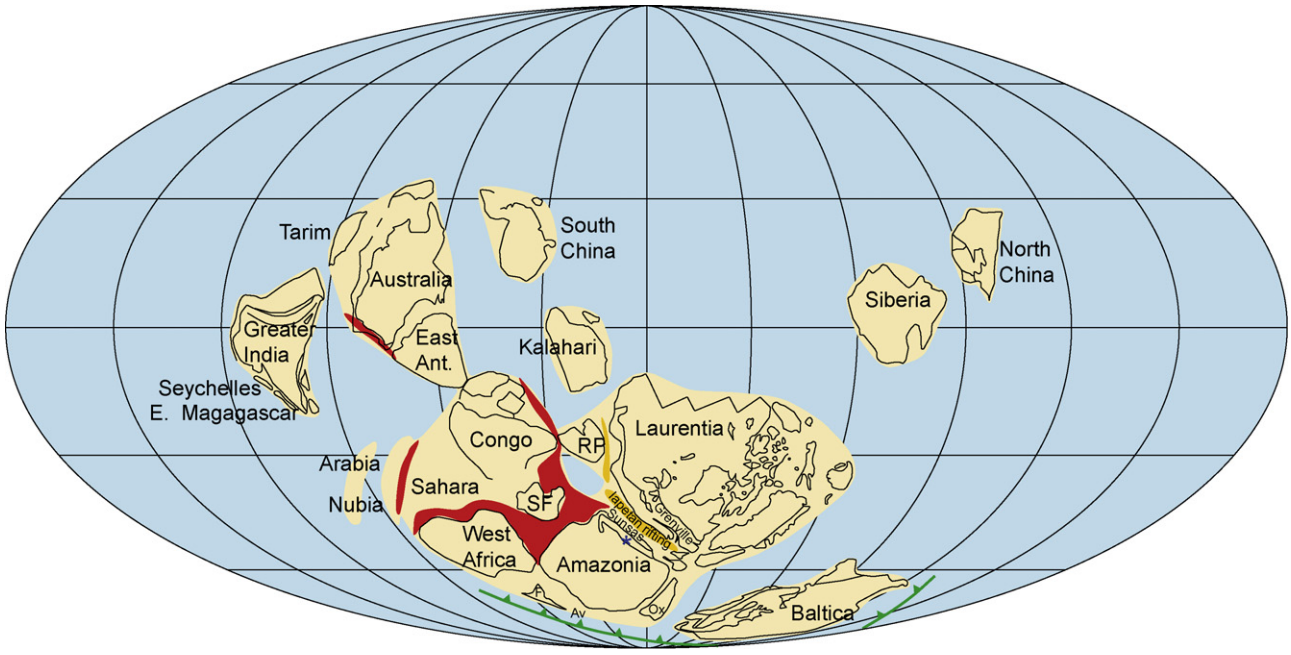

Fig. 1. Palaeogeographic reconstruction of Rodinia at 600 Ma modified from Li et al. (2008). In this reconstruction, western Amazonia (marked by a blue asterisk) is still attached to eastern Laurentia. Active magmatic belts at ca. 600 Ma are marked in red, proto-rifts (i.e. the birth of Iapetus Ocean) are marked in orange. RP = Rio de la Plata craton, SF = São Francisco craton, Ox = Oaxaquia., F = Florida, Av = Avalonia. (For interpretation of the references to color in the figure caption, the reader is referred to the web version of the article.)

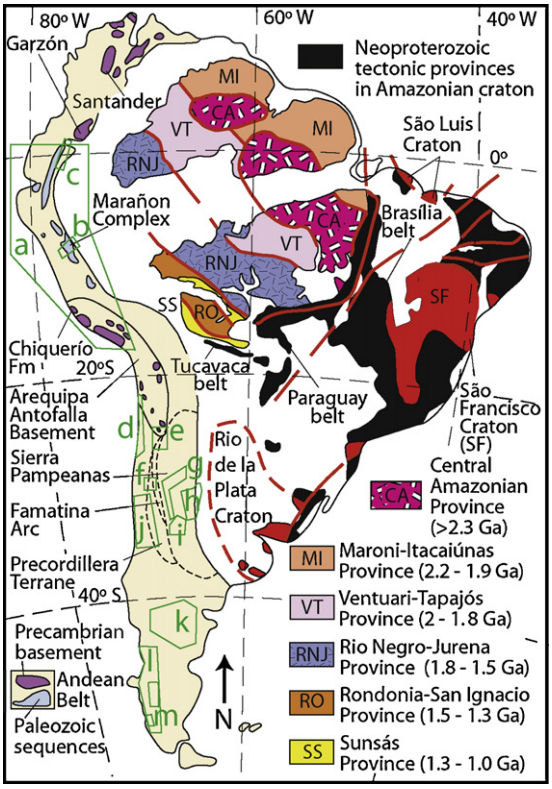

Fig. 2. Map of South America illustrating the major tectonic provinces and the ages of their most recent metamorphic events. Adapted from Cordani et al. (2000). Precambrian and Palaeozoic inliers in the Andean belt are shown in purple and light gray, respectively. Studies which have presented U–Pb detrital zircon data from the Proto-Andean margin are highlighted by lettered green boxes. (For interpretation of the references to color in the figure caption, the reader is referred to the web version of the article.)

of Precambrian basement rocks within the present-day Andean chain, and the difficulty in deciphering tectonic histories in rocks, which have experienced multiple orogenic events throughout the Phanerozoic. However evidence from segments of the Proto-Andean margin, particularly the Sierra Pampeanas, suggests that magmatic arc activity initiated from ca. 650 Ma to 530 Ma (Escayola et al., 2007; Rapela et al., 1998). This is substantially older than that observed on the conjugate margin of Laurentia, where there is no clear evidence for subduction-related magmatism older than 500 Ma on the margin (e.g. Dewey and Mange, 1999) or older than 510 Ma in peri-Laurentian arcs such as the Lushs Bight oceanic tract in Newfoundland (van Staal et al., 2007). In this paper we present new and previously published U–Pb zircon ages from clastic sedimentary rocks and from xenocrystic zircon cores in granitic rocks from the northern and central segments of the Proto-Andean margin. These data are used to infer the palaeogeography and tectonic evolution of the Proto-Andean margin from the break-up of Rodinia to the initiation of Iapetus Ocean closure.

2. Geological setting of the northern and central Proto-Andes

The boundary between the northern and central Proto-Andes is marked by a major structural lineament, the Huancabamba deflection (Fig. 3). To the north of the Huancabamba deflection, the Andes of Ecuador can be subdivided into a Western Cordillera consisting of accreted late Cretaceous oceanic rocks, and an Eastern Cordillera (the Cordillera Real) which consists of Mesozoic plutons emplaced into probable Palaeozoic metamorphic pelites and volcanics (Fig. 3). The southern boundary of the accreted oceanic rocks is marked by the Gulf of Guayaquil (Fig. 3). The metamorphic belts of the Cordillera Real continue into northern Peru (e.g. the Olmos Complex in Fig. 3), where the Huancabamba deflection defines a marked change in the orientation of the Andean chain at about 6°S.

South of the Huancabamba deflection, the Peruvian Andes are comprised of a Western Cordillera consisting of Mesozoic sedi-

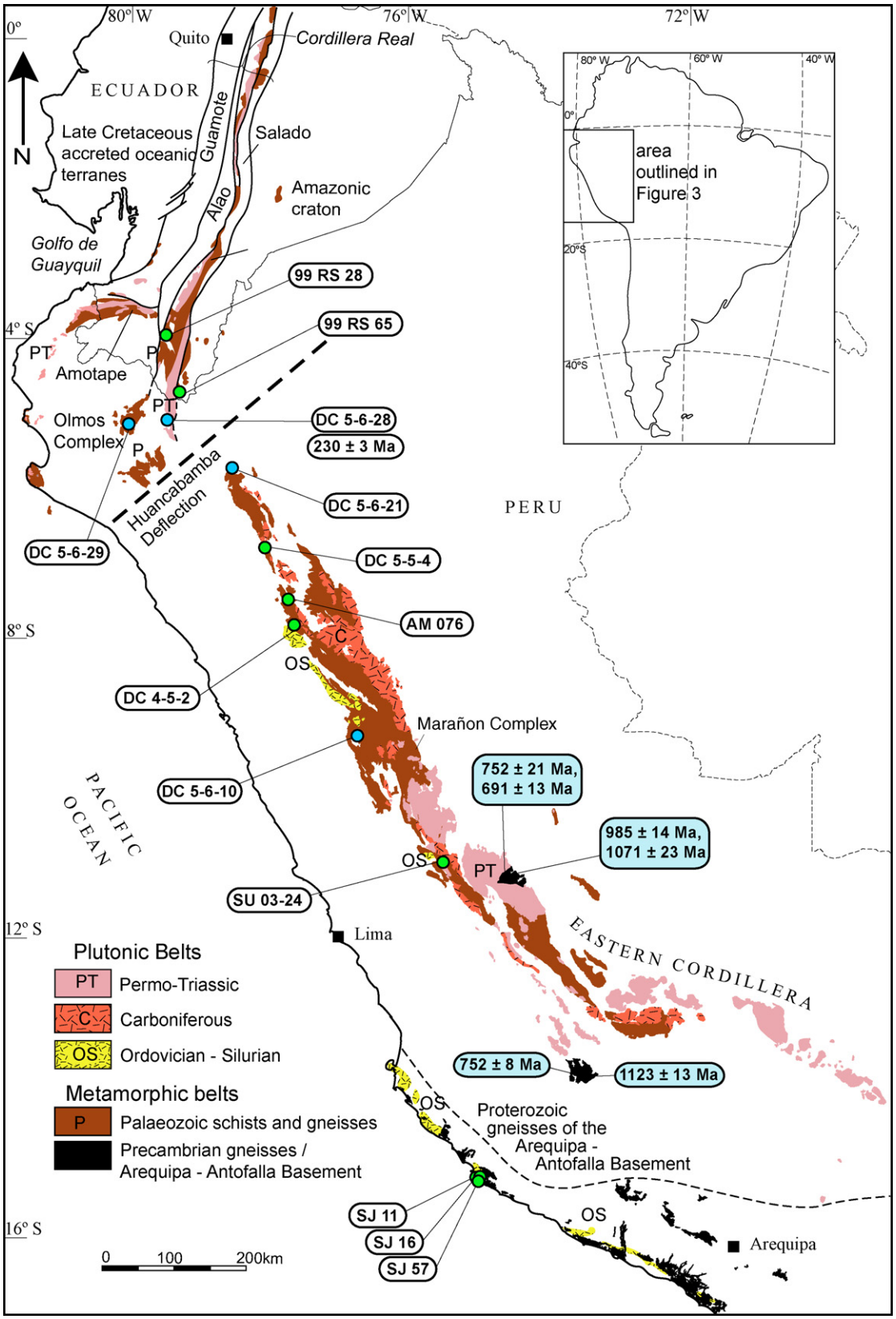

Fig. 3. Geological map of Peru and Ecuador illustrating the major Palaeozoic metamorphic and magmatic belts along with the Proterozoic gneisses of the Arequipa–Antofalla Block. Geology is adapted from Litherland et al. (1994) and Leon et al. (2000) and incorporates recent geochronological studies in the Eastern Cordillera of Peru (Chew et al., 2007a; Miškovic et al., in press). U–Pb zircon samples referred to in the text and in Fig. 4 are in white boxes; U–Pb zircon geochronological data from Miškovic et al. (in press) are in blue boxes. (For interpretation of the references to color in the figure caption, the reader is referred to the web version of the article.)

ments intruded by a Mesozoic arc (the Coastal Batholith) with younger Tertiary volcanics and localized plutons (the Cordillera Blanca). An Eastern Cordillera consists of a sequence of metasedimentary schists and gneisses (the Marañon Complex) intruded chiefly by Carboniferous and Permo-Triassic plutons (Fig. 3). The basement to the Western Cordillera north of 14° S is unexposed. It is believed to represent either extremely attenuated Cretaceous intra-arc basin floored by sialic crust with more than 9 km of mafic volcanics (Ramos, 2008) or accreted oceanic material (Polliand et al., 2005 and references therein). South of 14° S the coastal batholith is intruded into Proterozoic gneisses of the Arequipa-Antofalla Basement (Figs. 2 and 3).

2.1. Cordillera Real of Ecuador

There is sparse age control on the Palaeozoic metamorphic pelites and volcanics of the Cordillera Real of Ecuador, and opinion differs as to whether the majority of the units are allochthonous (e.g. Litherland et al., 1994), or autochthonous (e.g. Pratt et al., 2005). The uncertainty relates to the tectonic significance attached to north–south faults which run along the spine of the Cordillera Real. The model of Litherland et al. (1994) invokes these faults as major Mesozoic terrane-bounding sutures, which separate a series of suspect terranes. These are illustrated in Fig. 3 and are from west to east: Guamote (continental), Alao (island arc), Loja (continental), Salado (island arc) and Amazonic (continental craton). The model of Pratt et al. (2005) considers these units autochthonous as they share a similar structural history, while the majority of the major terrane-bounding sutures are re-interpreted as intrusive contacts between major plutons and pelitic units, which were reactivated during Andean tectonics. The major phase of fault movement in the region (which has apparent vertical displacements of many kilometres) is believed to be Miocene–Pliocene in age (Pratt et al., 2005).

2.2. Eastern Cordillera of Peru

Recent research has demonstrated the presence of a subduction-related magmatic belt (474–442 Ma) in the Eastern Cordillera of Peru (Chew et al., 2007a), while U–Pb ion microprobe dating of zircon overgrowths from amphibolite-facies schists (the Marañon Complex) has documented regional orogenic events which pre- and post-date this phase of magmatism at ca. 480 Ma (Chew et al., 2007a; Cardona et al., 2006, 2007), ca. 420 Ma (Cardona et al., 2007) and ca. 315 Ma (Chew et al., 2007a). These orogenic events are considered equivalent to the Early Ordovician Famatinian Orogeny (Pankhurst et al., 1998) and the Late Palaeozoic pan-Pacific Gondwanide Orogeny (Cawood, 2005), respectively (Chew et al., 2007a).

The timing of younger, Carboniferous–Jurassic, magmatism in the Peruvian Eastern Cordillera is now well constrained by a comprehensive U–Pb zircon dataset (Miškovic et al., in press). Two principal plutonic belts of Palaeozoic to Mesozoic age can be distinguished; Early Carboniferous I-type metaluminous to peraluminous granitoids, chiefly restricted to the segment north of 13° S and Permian to Early Triassic S to A-type granitoids in central and southern Peru (Fig. 3).

2.3. Arequipa–Antofalla Basement

The Arequipa–Antofalla Basement (AAB) crops out on the western coast of southern Peru and northern Chile (Fig. 2). It is comprised of three zones with Palaeoproterozoic (1.79–2.02 Ga) components in the north, Mesoproterozoic rocks in the central segment and Ordovician units in the south in northern Chile (Loewy et al., 2004). This southward trend of crustal growth disrupts an otherwise simple pattern in the Amazonian craton, which comprises a Palaeoproterozoic core with progressively younger domains toward the west (Fig. 1). Most authors have proposed that the Arequipa–Antofalla Basement is allochthonous to Amazonia (e.g. Ramos, 1988; Dalziel, 1994; Loewy et al., 2004). It was most likely accreted to Amazonia during the 1000–1300 Ma Grenville–Sunsas orogeny and the assembly of Rodinia (e.g. Loewy et al., 2004; Chew et al., 2007b). U–Th–Pb *in situ* electron microprobe dating of metamorphic monazite in the AAB in southern Peru yields ca. 1000 Ma ages, and are associated with regional UHT (>900 °C) assemblages that formed at pressures in excess of 1 GPa (Martignole and Martelat, 2003). The Arequipa–Antofalla Basement is locally overlain in southern Peru by the Chiquerío Formation, a tillite deposit of Neoproterozoic age (Chew et al., 2007b; Caldas, 1979). Detrital zircon geochronology from the Chiquerío Formation and C isotope chemostratigraphy of its overlying cap carbonate (the San Juan Formation) are consistent with the Chiquerío Formation being equivalent to the ca. 750–700 Ma Sturtian glacial event (Chew et al., 2007b). A comprehensive review of the geological evolution of the Arequipa–Antofalla Basement and the Early Palaeozoic metamorphic sequences of Peru, Bolivia and northern Chile and Argentina is provided by Ramos (2008).

3. U–Pb zircon data

The detrital zircon record of clastic sediments is an important provenance tool, which can link sedimentary basins to potential source regions. There is now a relatively comprehensive U–Pb detrital zircon database for the Proto-Andean margin, although this dataset is largely based on segments of the margin south of 20° S (Fig. 2). Given the limited amount of exposure of Precambrian basement rocks within the present-day Andean chain, these detrital zircon data provide valuable constraints on the palaeogeography and tectonic evolution of the Proto-Andean margin.

We provide examples of detrital zircon populations from autochthonous rocks from the northern and central segments of the Proto-Andean margin of South America (four new samples and nine recently published samples from the literature (Chew et al., 2007a,b, Fig. 3 (area a), Fig. 4a and b). The detrital zircon data were obtained from both sedimentary rocks and from xenocrystic cores in granitic and migmatitic rocks from the northern and central Andes. These inherited zircon cores offer additional provenance information, as they may transport xenocrystic zircon from deeper crustal levels that would otherwise be impossible to sample. The sedimentary samples span a broad range of depositional ages (Late Neoproterozoic to Lower Cretaceous), while the crystallization ages of the magmatic samples ranges from the Late Ordovician to the Middle Triassic. None of these sedimentary sequences, or any of the plutonic bodies are exotic to the Proto-Andean margin (Chew et al., 2007a). These data are compared to other published results from the northern and central Proto-Andes (Cardona et al., 2006 (Fig. 3, area b)) and Martin-Gombojav and Winkler, 2008 (Fig. 2a and c) and along with U–Pb detrital zircon data from Argentina and Chile (see later).

3.1. U–Pb detrital zircon data from the northern and central Proto-Andes

Analytical techniques are presented in Appendix A and all laser ablation ICPMS (LA-ICPMS) data along with secondary ion microprobe results are presented in the supplementary publication (see Appendix C). Secondary ion microprobe data for one sample (DC 5-6-28) are presented in Table 1. For comparison, all data are filtered according to the same rejection criteria which incorporates a filter

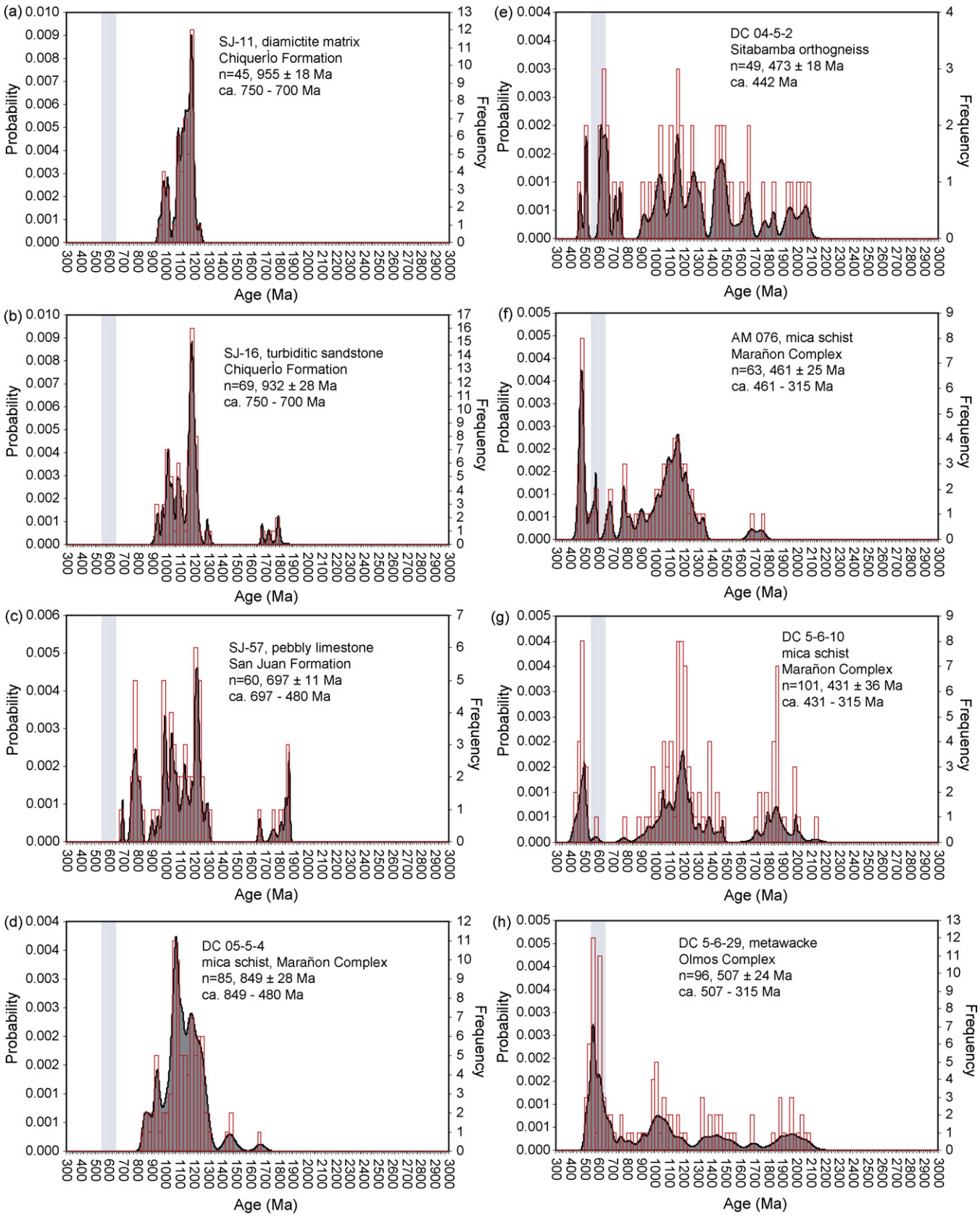

Fig. 4. (a–m) Zircon probability density distribution diagrams for both metasedimentary and magmatic (inherited cores) samples. Grey vertical band highlights the time period 550–650 Ma. (n and o) Tera-Wasserburg concordia diagrams showing zircon ages for sample DC 5-6-28 dated by ion microprobe. (n) Inherited cores and (o) zircon rims interpreted as dating migmatization. (p) Representative zircon petrography (SEM-CL) for ion microprobe analyses for sample DC 5-6-28. Sample identification of ion microprobe data points corresponds to Table 1, (m) and (n). All quoted ages are $^{206}Pb/^{238}U$ ages and uncertainties are at the 2σ level. All images use a 100 μm scale bar.

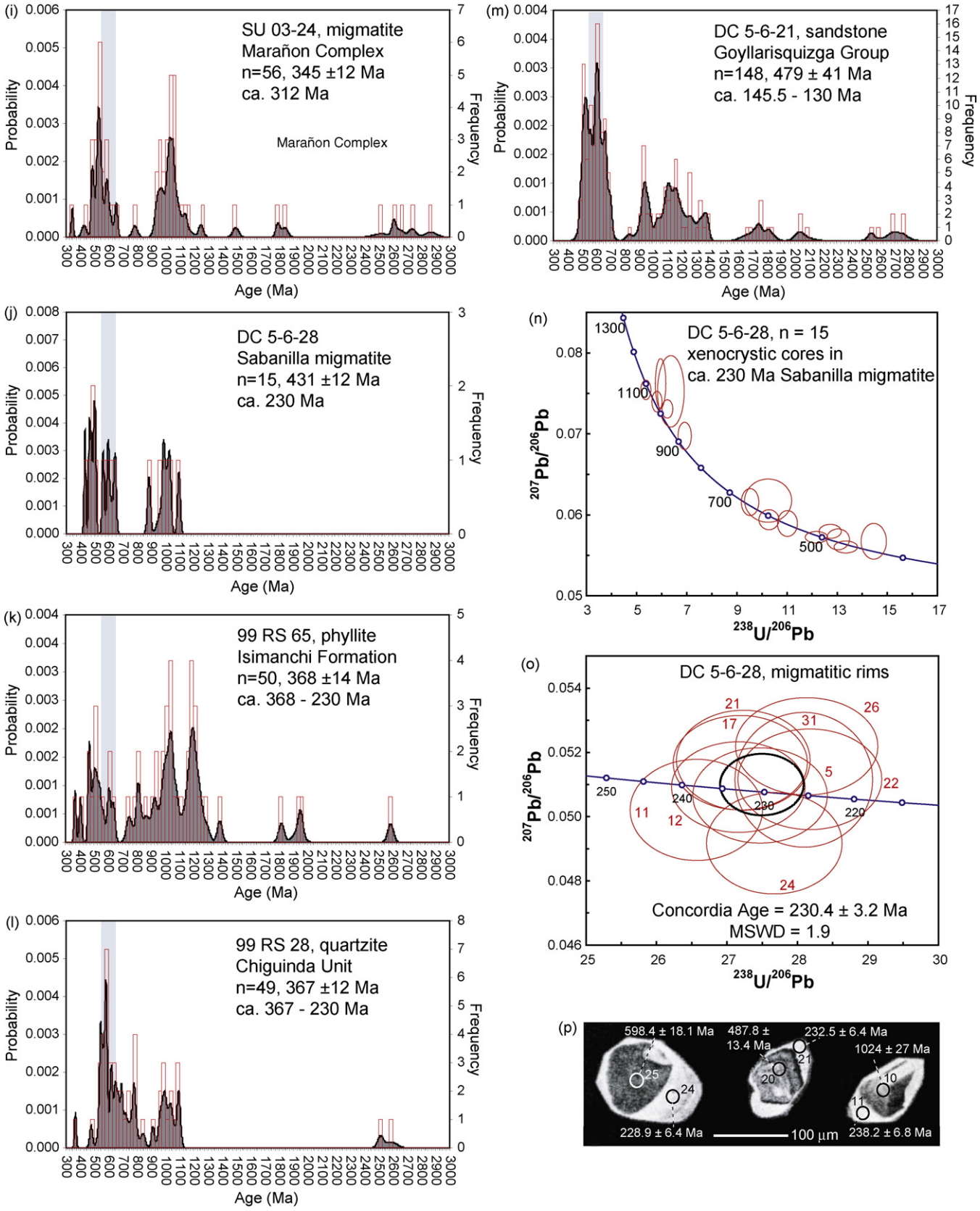

Fig. 4. (*Continued*).

Table 1
Ion microprobe U–Pb zircon data

Sample/spot	U (ppm)	Th (ppm)	Pb (ppm)	Th/U	f^{206} (%)	$^{238}U/^{206}Pb$	±σ%	$^{207}Pb/^{206}Pb$	±σ%	% Disc. (2σ)	$^{206}Pb/^{238}U$	Ma ± σ
DC 5-6-28 [17 M 684735 9410300]												
22 rim	415	3	16	0.010	{0.32}	28.18	1.5	0.05116	1.3		225	3
31 rim	399	3	15	0.008	{0.18}	28.09	1.4	0.05115	1.7		226	3
26 rim	460	3	17	0.008	{0.11}	28.13	1.5	0.05219	1.2	−2.30	225	3
24 rim	381	3	14	0.014	{0.23}	27.67	1.4	0.04917	1.3	1.61	229	3
5 rim	423	3	16	0.012	{0.20}	27.47	1.4	0.05066	1.2		231	3
21 rim	440	5	17	0.019	{0.32}	27.23	1.4	0.05175	1.2		232	3
12 rim	506	3	20	0.010	{0.22}	27.16	1.4	0.05092	1.1		233	3
17 rim	460	3	18	0.008	{0.06}	27.19	1.4	0.05168	1.2		233	3
11 rim	408	3	16	0.017	{0.11}	26.56	1.4	0.05021	1.3		238	3
2 core	147	185	15	1.121	{0.23}	14.46	1.4	0.05673	1.6		431	6
23 core	992	964	102	1.059	{0.09}	13.34	1.4	0.05603	0.5		466	6
30 core	289	474	35	1.657	{0.08}	13.03	1.4	0.05698	0.9		477	7
20 core	670	126	59	0.209	{0.07}	12.72	1.4	0.05796	0.6	−0.99	488	7
27 core	1739	1365	186	0.806	{0.00}	12.17	1.5	0.05724	0.5		509	7
8 core	176	118	20	0.679	{0.13}	11.02	1.5	0.05893	1.1		560	8
9 core	267	303	37	1.068	{0.34}	10.25	3.7	0.06176	1.8		600	22
25 core	722	93	77	0.137	{0.02}	10.28	1.6	0.05941	0.8		598	9
6 core	150	72	19	0.494	{0.03}	9.53	1.5	0.06158	1.1		643	9
14 core	282	71	47	0.247	{0.04}	6.92	1.6	0.06976	1.0		870	13
4 core	182	88	35	0.448	{0.05}	6.37	3.4	0.07527	2.4		940	30
19 core	245	113	48	0.455	{0.03}	6.23	1.4	0.07309	0.6	−1.05	960	13
13 core	43	12	8	0.271	{0.23}	5.96	1.4	0.07624	1.6		1000	13
10 core	372	106	75	0.293	{0.01}	5.81	1.4	0.07399	0.7		1024	14
18 core	218	235	57	1.143	0.06	5.37	1.5	0.07589	0.6		1101	16

UTM coordinates are given in square brackets after the sample number. f^{206} (%) is the percentage of common ^{206}Pb, estimated from the measured ^{204}Pb. Values in parentheses indicate that no correction has been applied owing to insignificant levels of ^{204}Pb. % Disc. (2σ) is the age discordance at the closest approach of the 2σ error ellipse to Concordia. All other errors are at the 1σ level. Age calculations use the routines of Ludwig (2003) and follow the decay constant recommendations of Steiger and Jäger (1977).

for both ($^{207}Pb/^{206}Pb$)/($^{206}Pb/^{238}U$) age discordance and large age uncertainties (<20% discordance of the centroid and a Concordia age with a 2σ uncertainty of less than 10%). All reported data are $^{206}Pb/^{238}U$ ages.

3.1.1. Pre-Famatinian (ca. 480 Ma) sequences

U–Th–Pb ion microprobe analyses of detrital zircons from three samples from the Chiquerío and San Juan Formations (a Neoproterozoic glacial unit and its overlying carbonate cover sequence, Fig. 3) were presented in Chew et al. (2007b). Combined age (probability–density–distribution) plots and histograms for the three samples are illustrated in Fig. 4a–c, along with detrital zircon data from the Marañon Complex in the Eastern Cordillera of Peru (sample DC 05-5-4, Chew et al., 2007a, Fig. 4d). This sample is included for comparison as it is a Gondwanan margin sequence (Chew et al., 2007a) that overlaps with the assumed depositional age range of the Chiquerío and San Juan Formations. This Marañon Complex sample is cut by ca. 480 Ma leucosomes (Chew et al., 2007a) and yields a youngest detrital zircon of 849 ± 28 Ma with the majority of the detritus lying in the 950–1300 Ma range. Sample SJ-11 (Fig. 4a, 45 grains) is from a thin graded turbiditic sandstone bed the Chiquerío Formation and yields a restricted age distribution between 950 Ma and 1300 Ma, with a prominent peak at ca. 1200 Ma and a subsidiary peak at ca. 1000 Ma. SJ-16 (Fig. 4b, 69 grains) is a sample of diamictite matrix from the Chiquerío Formation. It is also characterized by a restricted age distribution from 950 Ma to 1300 Ma, with a prominent c. 1200 Ma peak and a subsidiary c. 1000 Ma peak. The detrital zircon data from both samples from the Chiquerío Formation yield very minimal detritus (five grains between 1800 Ma and 1680 Ma in sample SJ-16) which could potentially be derived from the underlying basement, the Palaeoproterozoic (1790–2020 Ma) northern domain of the AAB (Loewy et al., 2004). Sample SJ-57 (Fig. 4c, 60 grains) is from a coarse pebbly limestone bed from the San Juan Formation, 1412 m above the Chiquerío Formation–AAB contact. The majority of grains from this sample also lie in the 950–1300 Ma range with peaks ca. 1000 Ma and ca. 1200 Ma. There are also minor peaks within the ca. 1600–2000 Ma and ca. 700–830 Ma intervals.

3.1.2. Syn-Famatinian (ca. 440 Ma) intrusives

Sample DC 04-5-2 is a strongly foliated granodiorite (the Sitabamba orthogneiss) with conspicuous augen of relic igneous plagioclase and development of metamorphic biotite and garnet. The Sitabamba orthogneiss intrudes the Marañon Complex in the southwest portion of the Marañon Complex outcrop in northern Peru (Fig. 3; Chew et al., 2007a; Wilson et al., 1995). Results of LA-ICPMS dating of inherited zircon cores within the Sitabamba orthogneiss were presented in Chew et al. (2007a) and are shown in Fig. 4e (49 grains). The youngest detrital zircon (473 ± 18 Ma) forms part of a small peak of ca. 480 Ma (Famatinian) detritus. Older peaks are encountered at 900–1350 Ma, 1400–1700 Ma and minor amounts of detritus from 1800 Ma to 2100 Ma (Fig. 4e). Sample DC 04/5–2 yielded U–Pb zircon isotope-dilution thermal ionization mass spectrometry (ID-TIMS) and LA-ICPMS crystallization ages of 442.4 ± 1.4 Ma and 444.2 ± 6.4 Ma, respectively (Chew et al., 2007a).

3.1.3. Post-Famatinian, pre-Gondwanide (ca. 440–315 Ma) sequences

Samples AM-076, DC 5-6-10 and DC 5-6-29 are greenschist-facies metawacke samples from the Marañon Complex (Fig. 3, samples AM-076, DC 5-6-10) and Olmos Complex (Fig. 3, sample DC 5-6-29), respectively. These units have been traditionally assigned to the Precambrian (e.g. Leon et al., 2000). Cardona et al. (2006) and Chew et al. (2007a) documented the presence of Famatinian detritus in the Marañon Complex demonstrating that at least part of this Complex was deposited in the Lower Palaeozoic. Sample AM-076 (63 grains, Fig. 4f) crops out in northern Peru (Fig. 3; Chew et al., 2007a) and yields a strong ca. 480 Ma Famatinian peak with a subsidiary peak in the 550 Ma age range. The majority of detritus lies in the 800–1350 Ma range, with a small peak around 1700–1800 Ma (Fig. 4f). Sample DC 5-6-10 (101 grains, Fig. 4g) is a new sample

from this study and crops out 200 km to the SSW (Fig. 3). It yields a virtually identical age spectrum to sample AM-076, with a prominent 480 Ma Famatinian peak and a minor peak in the 550 Ma age range. The majority of detritus lies in the 900–1350 Ma age range, with a small peak at 1700–2100 Ma (Fig. 4g). Sample DC 5-6-29 (96 grains, Fig. 4h) is also a new sample from the Olmos Complex. The youngest detrital zircon of 507 ± 24 Ma confirms that the Olmos Complex is Phanerozoic. It has a very prominent detrital peak in the 500–650 Ma age range, with smaller peaks at 900–1300 Ma, 1350–1600 Ma and 1800–2100 Ma (Fig. 4h). The youngest regional metamorphic event to affect the Marañon Complex (and by inference the Olmos Complex) in Peru is the ca. 315 Ma Gondwanide orogeny (Chew et al., 2007a), which provides the minimum depositional age limit for these three samples (Fig. 4f–h).

3.1.4. Syn-Gondwanide (ca. 312 Ma) intrusives

Sample SU 03–24 is a migmatic paragneisses in the Marañon Complex of the central portion of the Eastern Cordillera of Peru, which yielded a U–Pb zircon ion microprobe crystallization ages of 312.9 ± 3.0 Ma (Chew et al., 2007a). LA-ICPMS dating of inherited zircon cores within this paragneiss was presented in Chew et al. (2007a) and is reproduced in Fig. 4i (56 grains). The youngest detrital zircon is 345 ± 12 Ma. Prominent peaks are encountered at 500–650 Ma and 900–1200 Ma. There is a restricted amount of detritus in the 2500–2900 Ma age range (Fig. 4i).

3.1.5. Post-Famatinian–Middle Triassic (ca. 430–230 Ma) sequences

The Sabanilla migmatite crops out in southern Ecuador and northern Peru (Fig. 3). The age of metamorphism in northern Peru was inferred as Late Precambrian (Leon et al., 2000), whereas a Rb–Sr whole rock isochron of 224 ± 37 Ma has been obtained from the correlative sequence in southern Ecuador (Litherland et al., 1994). Sample DC 5-6-28 is a new sample from the Sabanilla migmatite. Ion microprobe dating of xenocrystic cores (15 grains, Fig. 4j, Fig. 4n, Table 1) yields three populations at 430–500 Ma, 550–650 Ma and 850–1100 Ma. The crystallization age of the migmatite is constrained by a U–Pb zircon ion microprobe Concordia age of 230.4 ± 3.2 Ma (Fig. 4o, Table 1). Sample 99 RS 65 (50 grains, Fig. 4k) crops out in southern Ecuador (Fig. 3; Chew et al., 2007a), and is a phyllite from the Isimanchi Formation, which forms part of the Amazonian cratonic cover. It consists of very low-grade phyllites and marbles and has a poorly constrained Carboniferous–Late Triassic age based on fish remains (Litherland et al., 1994). It yields a minor peak in the 350–400 Ma age range and has also grains between 500 Ma and 650 Ma. The majority of detritus lies in the 800–1350 Ma age range. Furthermore, minor peaks at 1800–2000 Ma and one grain at 2600 Ma define the complete population (Fig. 4k). Sample 99 RS 28 (49 grains, Fig. 4l) crops out in southern Ecuador (Fig. 3; Chew et al., 2007a). It is a quartzite from the Chiguinda Unit, part of the presumed allochthonous Loja terrane of Litherland et al. (1994). This unit consists of quartzites and black phyllites of poorly constrained age thought to be post-Silurian based on miospore data (Litherland et al., 1994). It yields a small peak at 350 Ma, a significant peak in the 500–800 Ma age range, a minor 900–1100 Ma peak and has a minor constituent of 2500–2700 Ma grains (Fig. 4l). The age of the regional metamorphic event to affect these two metasedimentary samples (99 RS 65 and 99 RS 28) is not known. The ca. 230 Ma tectonothermal event which affected the Sabanilla migmatite is believed to represent the age of metamorphism and hence the inferred minimum depositional age for these two samples (Fig. 4k and l).

3.1.6. Lower Cretaceous (ca. 145.5–130 Ma) sequences

Sample DC 5-6-21 (148 grains, Fig. 4m) is a new sedimentary sample from the Goyllarisquizga Group, which overlies the Marañon Complex in northern Peru (Fig. 3). It was deposited during the Neocomian (Lower Cretaceous) (Carrascal-Miranda and Suárez-Ruiz, 2004) which corresponds to a depositional age of 145.5–130 Ma using the timescale of Gradstein et al. (2004). There is a very prominent peak at 500–700 Ma, a peak at 900–1400 Ma and minor contributions from 1600–1900 Ma, 2000–2100 Ma and 2500–2800 Ma grains (Fig. 4m).

3.2. Dataset synthesis

The majority of samples exhibit a prominent peak between 450 Ma and 500 Ma, and the most likely source is a subduction-related magmatic belt in the Eastern Cordillera of Peru (Chew et al., 2007a), similar to the Famatinian arc of central Argentina (Pankhurst et al., 1998). A second prominent peak is encountered between 900 Ma and 1300 Ma. The most likely source for this population is the Sunsas orogen of the Southwest Amazonian craton which probably lies beneath the Northern and Central Andean foreland basins and is contiguous with the ca. 1 Ga gneissic basement inliers in the Columbian Andes (Restrepo-Pace et al., 1997). The Arequipa–Antofalla Basement in southern Peru and northern Chile is comprised mainly of Palaeoproterozoic gneisses (Loewy et al., 2004) and is unlikely to be a large source of detritus in the 900–1300 Ma age range. Most samples yield minimal detritus older than 2000 Ma.

However, the source of detritus in the 550–650 Ma age range is very important as there is little evidence on the western Gond-

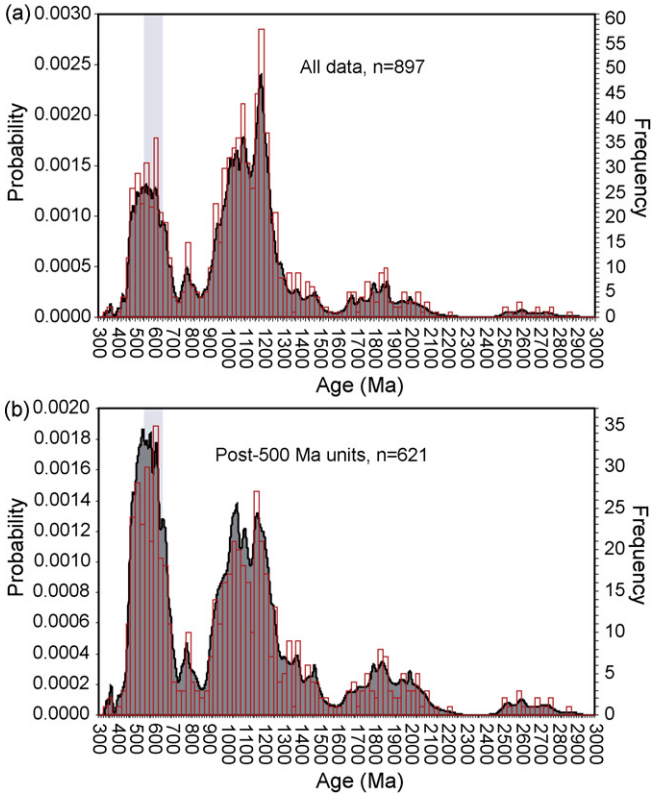

Fig. 5. (a) Composite zircon probability density distribution diagrams for all metasedimentary and magmatic (inherited cores) samples in Fig. 4a–m. (b) Composite zircon probability density distribution diagrams for syn–post Famatinian (i.e. post 500 Ma) metasedimentary and magmatic (inherited cores) samples in Fig. 4e–m. Grey vertical band highlights the time period 550–650 Ma in both figures.

wanan margin for magmatism at this time. This is discussed in detail later in Sections 4 and 5. Fig. 5a combines all data from this study (897 grains) and yields similar trends to those described above from the individual samples. The major peaks are at 450–650 Ma and 900–1300 Ma while minor peaks of older detritus are at 1650–2100 Ma and 2500 Ma–2900 Ma. Some samples (the Pre-Famatinian samples SJ-11, SJ-16, SJ-57 and DC 05-5-4) do not exhibit any detritus younger than 700 Ma. This is consistent with their envisaged depositional age being too old to have accumulated detritus in the 550–650 Ma age range. Removing these four samples from the combined dataset (Fig. 5b, 621 grains) reveals an even more prominent peak in the 450–650 Ma age range.

3.3. Comparison with other U–Pb detrital zircon datasets from the northern and central Proto-Andes

The dataset for the northern and central Proto-Andes is restricted compared to the southern segments of the margin. Cardona et al. (2006, 2007) presented U–Pb LA ICPMS and SHRIMP detrital zircon data from Palaeozoic sequences in the Huanuco–La Union region in the Eastern Cordillera of Peru (10° S, Fig. 2, area b). Of the 514 analyzed grains, the two most important detrital zircon populations ranged between 490–620 Ma and 1000–1400 Ma, with 40% of all analyzed grains falling in the 490–620 Ma age range and 36% of all analyses falling in the 1000–1400 Ma age range. This trend is very similar to the results discussed previously in Fig. 5a and b. Martin-Gombojav and Winkler (2008) presented U–Pb LA ICPMS detrital zircon data from five formations (ranging from the Middle Cretaceous–Oligocene) from the sub-Andean zone east of the Cordillera Real in Ecuador (Fig. 2, area c). Interestingly, detritus in the 450–650 Ma age range is most abundant in the oldest sample analyzed (comprising 21% of detritus in the Middle Cretaceous Hollin Formation), decreasing to 12% in the Eocene Tiyuyacu Formation and comprising only 2% of detritus in the Oligocene Chalcana Formation. The significance of this gradual reduction of detritus in the 450–650 Ma age range with decreasing stratigraphic age is discussed later.

3.4. Comparison with other U–Pb detrital zircon datasets from the southern Proto-Andes

There is now a substantial detrital zircon dataset for the southern portions of the Proto-Andean margin (Fig. 2, areas d–l). This review will consider each of these datasets in turn from north to south. Bahlburg and Vervoort (2007) presented LA ICPMS U–Pb detrital zircon data from Late Palaeozoic turbidite units of the Chilenia terrane in northern Chile (Fig. 2, area d). All samples essentially showed a similar distribution in detrital zircon populations, with populations directly corresponding to the "Grenvillian" orogenic cycle (1000–1400 Ma), the "Brasiliano" cycle at 550–800 Ma and an Early Palaeozoic Famatinian active margin between 420 Ma and 550 Ma. U–Pb detrital zircon ages from turbidite successions of the low grade Puncoviscana Formation show a dominant age component from 500 Ma to 650 Ma with minor populations at 900–1050 Ma and 1800–1900 Ma (Adams et al., 2007, Fig. 2, area e). In contrast, the U–Pb detrital zircon data of Thomas et al. (2004) from Cambrian synrift sequences in the Cuyania terrane (Fig. 2, area f) do not yield any components younger than Grenville. These detrital zircon data are consistent with previous interpretations that the Cuyania Terrane was rifted off Laurentia during Early Cambrian time and transferred to the western Gondwanan margin (Ramos et al., 1986; Ramos, 2004 and references therein). East of the Eastern Cordillera in the Sierra Pampeanas, sedimentary protoliths are dominated by Neoproterozoic (broadly 600 Ma) and late Mesoproterozoic (broadly 1100 Ma) detrital zircon (Rapela et al., 2007, Fig. 2 area g; Escayola et al., 2007, Fig. 2 area h; Steenken et al., 2006, Fig. 2 area i). Detrital zircon analyses from Late Palaeozoic accretionary complex rocks from latitudes 31° to 36° S (Willner et al., 2007, Fig. 2 area j) yield a similar pattern, with ages clusters between 390–580 Ma and 1000–1400 Ma. The southernmost datasets from the Proto-Andean margin come from the Patagonian Andes. U–Pb zircon age patterns for metasedimentary samples from NE Patagonia yield peaks at 550–750 Ma and 900–1200 Ma (Pankhurst et al., 2006, Fig. 2 area k). Further south, Late Palaeozoic metasediments yield detrital zircon age peaks at 350–700 Ma and 900–1500 Ma (e.g. Augustsson et al., 2006, Fig. 2 area l; Hervé et al., 2003, Fig. 2 area m).

4. Interpretation

The combined detrital zircon age spectra presented in Fig. 5a and b for the north-central segment of the Proto-Andean margin (Fig. 2 area a; Fig. 3) appear to be representative of most Palaeozoic units along the entire Proto-Andean margin, with the exception of the Laurentian Cuyania terrane (Thomas et al., 2004). The majority of samples (both from this study and previously published samples) exhibit a prominent peak between 450 Ma and 650 Ma, and a second significant peak is encountered between 900 Ma and 1300 Ma (Fig. 5a and b). The subdivision of the 450–650 Ma peak into two separate zircon populations (a late Neoproterozoic—early Cambrian source and a Late Cambrian to Ordovician source) is discussed later. In the north-central Proto-Andes (Fig. 2, area a), minor peaks are encountered at 1700–2000 Ma, and most samples yield minimal detritus older than 2000 Ma. With the exception of the Cuyania terrane, the only other samples which yield restricted detritus in the 450–650 Ma age range are from the Tertiary Amazonian foreland basin in Ecuador. There is a marked reduction in the amount of Late Neoproterozoic detritus from the Eocene to the Oligocene (Martin-Gombojav and Winkler, 2008), which temporally overlaps with the main phase of crustal shortening in the northern Central Andes (the middle Eocene to early Oligocene Incaic phase, Ramos and Aleman, 2000).

In the north-central segment of the Proto-Andean margin, a local source for the majority of detrital zircon crystals can be inferred. The most likely source for detrital zircon in the 450–500 Ma age range is a subduction-related magmatic belt in the Eastern Cordillera of Peru (Chew et al., 2007a, Fig. 3), similar to the Famatinian arc of northern Argentina (Pankhurst et al., 1998). The prominent peak encountered between 900 Ma and 1300 Ma was most likely sourced from a Grenvillian age orogen, which in the Southwest Amazonian craton is represented by Sunsas–Rondonian–San Ignacio Orogen (Tassinari and Macambira, 1999). It most likely lies beneath the Northern and Central Andean foreland basins, as suggested by the presence of a granulite inlier of possible Grenvillian age (U–Pb bulk unabraded zircon upper intercept age of 1140 ± 30 Ma) in the Peruvian Amazon Basin, east of Cuzco (Dalmayrac et al., 1980). This Mesoproterozoic orogenic belt extends to the northern Colombian Andes, where several ca. 1.25 Ga basement inliers, which initiated as arcs on the margins of the Amazon Craton have experienced ca 1 Ga metamorphism (Cordani et al., 2005; Restrepo-Pace et al., 1997). However detritus in the 500–650 Ma age range (Fig. 5a and b) is very abundant, yet has no obvious source in the Proto-Andean margin. Three options for the source of this prominent detrital peak are considered in detail below.

4.1. Origin of Neoproterozoic detrital zircon—derivation from the Brasiliano orogen?

The South American craton contains a large volume of Neoproterozoic orogenic belts, which developed in response to the

convergence of Amazonia and São Francisco cratons and other crustal blocks during the final assembly of western Gondwana. Referred to as the "Brasiliano orogenic collage" by de Brito Neves et al. (1999), these orogenic belts could potentially be the source of the abundant Neoproterozoic detrital zircon peaks encountered in the Proto-Andean margin. However, the south-westward extensions of the Brasiliano orogeny (i.e. those in closest proximity to Proto-Andean margin such as the Paraguay Belt and the Tucavaca Belt of Bolivia, Fig. 2) are predominantly deformed sedimentary successions (0.6–0.5 Ga, Pimentel et al., 1999) with no evidence of consumption of oceanic lithosphere. Deposition of these sequences may therefore have been in an intra-continental setting, possibly an aulacogen (Trompette, 1997) which was then deformed and metamorphosed in the Early Cambrian (Pimentel et al., 1999). The lack of calc-alkaline magmatism in the Paraguay and Tucavaca Belts means they cannot be a large source of detritus for the time period in question. Therefore the most plausible source of Neoproterozoic detrital zircon in the Brasiliano orogens is likely to be the N–S trending Brasília belt (Fig. 2) which contains both 0.8–0.7 Ga syn-collisional granitoids and 0.9–0.63 Ga arc meta-tonalites and meta-granodiorites (Pimentel et al., 1999). However, it is difficult to envisage how the Brasília belt can be a source to the Early Palaeozoic basins of the western Gondwanan margin as there is very minimal detritus from the intervening Amazonian craton. The cratonic nucleus of Amazonia (the Central Amazonian Province) is >2300 Ma old (Tassinari and Macambira, 1999), and this province was not a source of detritus in any pre-Carboniferous units in the northern and central Proto-Andes (e.g. Fig. 4a–h). If the Brasília belt was the source of the Neoproterozoic detrital zircon in the Proto-Andes, the Amazonian cratonic nucleus must have effectively behaved as a "ghost craton" (possibly due to peneplanation), not contributing in any significant amount to the Proto-Andean marginal sequences.

At present this is a difficult question to answer, as there are no palaeoelevation or burial history data for the Brazilian shield for this time period (the late Neoproterozoic). The cratonic nucleus of South America was generated by three complex Proterozoic tectonic events (de Almeida et al., 2000): the Paleoproterozoic Trans-Amazonian event, a mid to late Mesoproterozoic event (1400–950 Ma) responsible for the formation of Rodinia, and the final collage of the Gondwana supercontinent during the Late Neoproterozoic (the Brasiliano Orogenic cycle outlined above). The Phanerozoic evolution of the craton is characterized by a change to cratonic stability, with large sedimentary basins developing on a wide cratonic platform from the Ordovician to Permian periods, particularly during the Silurian (de Almeida et al., 2000). Available data therefore do not suggest partial burial of the cratonic nucleus until the Ordovician/Silurian.

4.2. Origin of Neoproterozoic detrital zircon—rift-related magmatism?

Another possible source of Neoproterozoic detrital zircon in the Proto-Andes is the rift-related magmatism associated with the break-up of Rodinia. A-type orthogneisses of mid Neoproterozoic age (774 ± 6 Ma) have been documented from the Grenvillian basement of the Precordillera terrane (Baldo et al., 2006). Similar ages (691 ± 13 Ma, 752 ± 8 Ma and 752 ± 21 Ma, Fig. 3) have been obtained for three foliated A-type granites from the Eastern Cordillera of Peru (Miškovic et al., in press). The youngest recorded extensional Neoproterozoic magmatic event in the Andean basement is a ca. 570 Ma syenite–carbonatite body reported from a Grenville-age terrane in the Sierra de Maz in the Western Sierras Pampeanas (Casquet et al., in press). However the majority of these ages (ca. 775–690 Ma) correspond to a very minor peak in the detrital zircon record (Fig. 5a and b) in the northern and central Proto-Andes, and are too old to be a source of the abundant Late Neoproterozoic detrital zircon encountered on the Proto-Andean margin which is 650–550 Ma. All younger Neoproterozoic extensional magmatism on the Proto-Andean margin is primarily basic in nature (Omarini et al., 1999) and is therefore unlikely to be a significant source of zircon as zircon usually crystallizes from felsic–intermediate magmas (e.g. Hoskin and Schaltegger, 2003). Juvenile extensional magmatism (dacitic dykes) has been dated at 635 ± 4 Ma in the Arequipa–Antofalla Basement of Northern Chile (Loewy et al., 2004). This rifting event probably involved the partial detachment of the Arequipa–Antofalla Basement (Loewy et al., 2004). Extension-related volcanism associated with Rodinia breakup has been identified in the Puncoviscana fold belt of northwestern Argentina (Omarini et al., 1999). This volcanism is undated, and the synrift products are ultra-potassic and alkaline basalts flows, which pass upwards into a thick sequence of pillow lavas of MORB affinity (Omarini et al., 1999). Ramos (2008) attributes the opening of the Puncoviscana basin with its mafic rocks of oceanic affinity to the separation of the Antofalla terrane from the Proto-Andean margin in the Late Neoproterozoic.

4.3. Origin of Neoproterozoic detrital zircon—an unrecognized Neoproterozoic active margin in the Proto-Andes?

There is a limited amount of Late Neoproterozoic basement presently exposed on the Proto-Andean margin. Recent research (Cardona et al., 2006; Chew et al., 2007a) has demonstrated that the Late Neoproterozoic *metamorphic* age assigned to granulitic gneisses of the Marañon Complex in Eastern Cordillera of central Peru (Dalmayrac et al., 1980) is erroneous, and that the Marañon Complex has instead experienced younger metamorphic events at ca. 480 Ma and ca. 315 Ma (Chew et al., 2007a). However, a Late Neoproterozoic *magmatic* belt (of uncertain extent) may be present in the northern and central Andes. Cardona et al. (2006) have suggested the existence of a ca. 620 Ma plutonic remnant within the Marañon Complex of the Eastern Cordillera of Peru, while Burkley (1976) obtained ages of ca. 650–580 Ma for autochthonous granitoids in the Venezuelan Andes. The Puncoviscana basin in the Puna and adjacent Eastern Cordillera of northwestern Argentina and southernmost Bolivia opened as a response to Neoproterozoic extension and the separation of the Antofalla terrane (Ramos, 2008). Early Cambrian calc-alkaline magmatism subsequently occurred in the Puncoviscana basin (Bachmann et al., 1987), and probably resulted from the Neoproterozoic extension being sufficiently large to allow subsequent subduction (Ramos, 2008). In the eastern Sierra Pampeanas, the existence of a late Neoproterozoic magmatic arc has long been proposed (Ramos, 1988). Escayola et al. (2007) have documented the presence of ophiolitic remnants of a Neoproterozoic back arc basin in the Eastern Sierra Pampeanas (Fig. 2, area g). These ophiolitic rocks have yielded a 647 ± 77 Ma Sm–Nd whole rock isochron. Escayola et al. (2007) suggest that a Neoproterozoic magmatic arc developed in between the Grenvillian basement of the Sierra Pampeanas and the Rio de la Plata Craton, and infer it to be the source area for the prominent 600–700 Ma detrital zircon peak seen in Pampean metasediments. Rapela et al. (2007) presented geochronological data from deep boreholes in western Argentina that penetrated Palaeozoic cover into basement of the Palaeoproterozoic (ca. 2 Ga) Rio de la Plata Craton. The location of the boreholes, some of them adjacent to the eastern limits of the Sierras Pampeanas, suggests that the Palaeoproterozoic crust extends further westwards than previously thought, leaving little room for any other form of basement province (e.g. the "Chaco terrane" of Keppie and Bahlburg (1999) or the magmatic arc of Escayola et al. (2007). Rapela et al. (2007) infer that the detritus which fed the Proto-Andean sequences in the Sierra

Pampeanas were exotic to the margin, probably derived from the 680 Ma to 540 Ma Dom Feliciano and 1000 Ma Namaqua–Natal belts.

However a similar model invoking exotic sources for Neoproterozoic detritus is not applicable to the northern and central segments of the Proto-Andean margin. In particular the prominent 900–1300 Ma peak seen in the detrital zircon record (Fig. 5a and b) can be best explained by derivation from the Sunsas Orogen or Grenvillian basement inliers such as the ca. 1140 Ma granulite inlier in the Amazon Basin of Eastern Peru (Fig. 2) which is the only orogen of Grenvillian age close to the north-central Proto-Andean margin. As described earlier, the only plausible presently exposed source for the 500–650 Ma detrital zircon peak (Fig. 5a and b) is the Brasília belt (Fig. 2), and this would imply that the Amazonian cratonic nucleus must have been effectively peneplained, not contributing in any significant amount to the Proto-Andean marginal sequences. As stated previously, while this option cannot be ruled out, there is no evidence for partial burial of the Amazonian cratonic nucleus until the Ordovician/Silurian, which corresponds to the initiation of deposition of the cover of the South American platform (de Almeida et al., 1999). Instead we propose that the voluminous 500–650 Ma detrital zircon peak is best explained by a proximal source to the north-central Andean margin, perhaps a continuation of the ca. 650–580 Ma basement of eastern Venezuela (Burkley, 1976; Marechal, 1983). This basement is inferred to subcrop under the present-day Amazonian foreland. It was probably covered during the Eocene–Oligocene, which temporally overlaps with both the disappearance of Neoproterozoic zircon in the detrital record of the Amazonian foreland (Martin-Gombojav and Winkler, 2008) and also with the main phase of crustal shortening in the northern Central Andes (the middle Eocene to early Oligocene Incaic phase, Ramos and Aleman, 2000). To produce an abundant supply of zircon, this inferred basement would have to contain a voluminous suite of acidic plutons, and most likely would have been produced at an active margin. The tectonic implications of such an orogenic belt are examined in the following section.

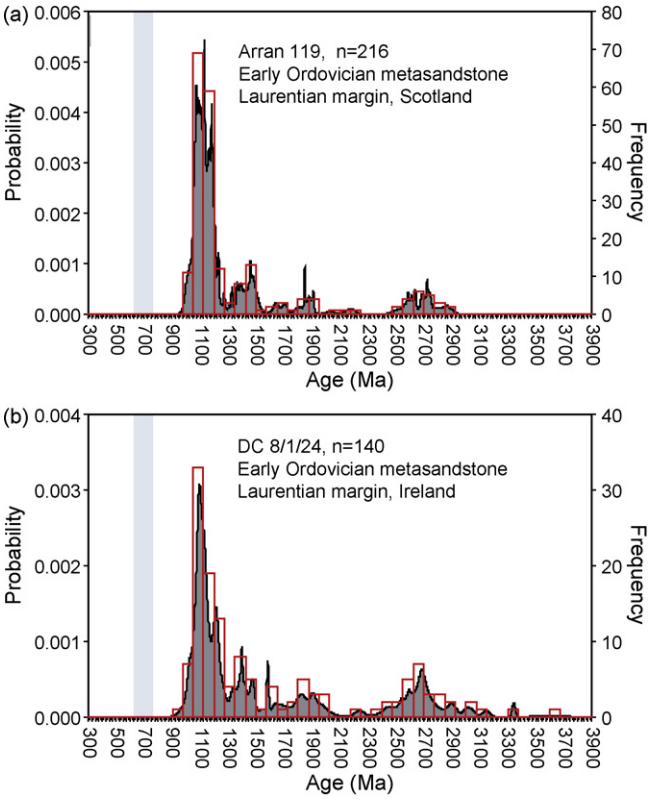

Fig. 6. (a) Zircon probability density distribution diagrams for two Ordovician metasedimentary samples from the Laurentian margin; (a) Scotland, (b) NW Ireland. Grey vertical band highlights the time period 550–650 Ma in both figures.

5. Tectonic implications

One of the enigmas of the early evolution of the Proto-Andean margin compared to its putative conjugate rifted margin of eastern Laurentia is the timing of the onset of subduction-related magmatism. Segments of the Proto-Andean margin were a destructive margin by ca. 650 Ma (e.g. Escayola et al., 2007 which is substantially older than eastern Laurentia, where there is no clear evidence for subduction-related magmatism older than 510 Ma (e.g. van Staal et al., 2007). This study puts forward evidence based on the detrital zircon record that a magmatic arc was sited on the northern segments of the Proto-Andean margin in Late Neoproterozoic time.

Comparing the detrital zircon record of Early Palaeozoic sequences on Laurentia (e.g. Cawood et al., 2007; Fig. 6, this study) with the Early Palaeozoic units in this study (e.g. Fig. 4a–h) reveals that both the Proto-Andean margin and Early Palaeozoic sequences in the U.S. Appalachians, Newfoundland and distal Laurentian margin sequences in Scotland and Ireland are dominated by ca. 1.1–1.0 detritus with very few pre-Mesoproterozoic grains (Cawood et al., 2007). Cawood et al. (2007) suggests that the prevalence of Grenville grains in many of the Eastern Laurentian margin sequences implies that the Grenville orogenic belt in these areas may have constituted a topographic barrier that limited sediment input from the older cratonic interior. A similar scenario was invoked by Chew et al. (2007a) to explain the abundance of Grenville-age detritus and lack of older grains on the Proto-Andean margin. Late Neoproterozoic zircons grains are a very minor component on eastern Laurentia (e.g. Cawood et al., 2007; Fig. 6, this study), yet constitute a very large peak on the Proto-Andean margin (Fig. 6a and b). The very minor component of late Neoproterozoic zircon grains (ca. 620–550 Ma) on eastern Laurentia is interpreted by Cawood et al. (2007) to have been derived from mafic-dominated, generally zircon-poor magmatic activity associated with the opening of Iapetus.

Two pulses of rifting activity, from ca. 760 Ma to 680 Ma and from ca. 620 Ma to 550 Ma, are recognized along the eastern margin of Laurentia (e.g. Aleinikoff et al., 1995; Tollo et al., 2004; Kamo et al., 1989; Cawood et al., 2001). The latter pulse is conventionally regarded to have resulted in the separation of Laurentia and cratonic elements of west Gondwana (e.g. Hoffman, 1991; Cawood et al., 2001; Li et al., 2008), followed by continued rifting along Laurentia's Iapetan margin, which generated a series of terranes at 540–535 Ma followed by Early Cambrian drift-related sedimentation (Williams and Hiscott, 1987). While some of these terranes, such as the Precordillera, left Laurentia, most like the Dashwoods Block in Newfoundland (Waldron and van Staal, 2001) subsequently returned to the Laurentian realm during subsequent orogeny.

However recent palaeomagnetic data (McCausland et al., 2007) suggest that Laurentia was already well separated from the Proto-Andean margin in Late Neoproterozoic time, although palaeomagnetic data for Amazonia during the Late Neoproterozoic (e.g. Trindade et al., 2003) are admittedly sparse. Waldron and van Staal (2001), Cawood et al. (2001) and van Staal et al. (2007) present geological evidence that implies that that the unequivocal ca. 550 Ma rifting event that occurred along Laurentia's Iapetan margin did not represent the separation of true cratons from Laurentia, but rather that of peri-Laurentian Appalachian basement terranes.

Additionally, the rift-drift transition in the early Palaeozoic clastic platform of the Proto-Andean margin which is constrained as Late Cambrian in northern Argentina to Early Ordovician in Peru (Ramos, 2008), is significantly too young to record the initiation of the separation of Laurentia from Gondwana, and may therefore record the separation of peri-Gondwanan basement terranes from the Proto-Andean margin.

If the unequivocal ca. 550 Ma rifting event that occurred along Laurentia's Iapetan margin did not represent the separation of true cratons from Laurentia, the possibility remains that the Iapetus Ocean began to open as early as ca. 750 Ma (McCausland et al., 2007), and that its formation could be contemporaneous with early pulses of magmatism along Laurentia's proto-Iapetan margin. This dominantly A-type felsic magmatism within the southern Appalachians (760–680 Ma) (Aleinikoff et al., 1995; Tollo et al., 2004) can now be demonstrated to have temporal counterparts (775–690 Ma) on the Proto-Andean margin (Baldo et al., 2006; Miškovic et al., in press, Fig. 2), and may have represented an initial intra-cratonic rift which developed true oceanic crust at ca. 700 Ma in the vicinity of the southern Appalachians and segments of the Proto-Andean margin. Subsequent consumption of this oceanic lithosphere on the Proto-Andean side of the ocean would have resulted in an active margin at around 650 Ma, which was then subsequently unroofed to feed detritus into the Early Palaeozoic Proto-Andean sequences.

This inferred Neoproterozoic magmatic arc temporally overlaps with the evolution of several peri-Gondwanan terranes, which have been interpreted as intra-oceanic arcs that were accreted onto the northern margin of the Amazon Craton (Fig. 1) from ca. 650 Ma onwards (e.g. Murphy et al., 2000, 2004a). The magmatic and detrital records of these peri-Gondwanan terranes, such as Avalonia, Ganderia, Florida, Carolina and Iberia, overlap with the Neoproterozoic-Cambrian and the Grenvillian sources feeding the Proto-Andean margin (Keppie et al., 1998; Ingle et al., 2003; Gutiérrez-Alonso et al., 2003; Collins and Buchan, 2004; Murphy et al., 2004b; Reusch et al., 2004; Carter et al., 2006; Rogers et al., 2006). The precise location of accretion of these terranes along the Gondwanan margin remains poorly constrained (e.g. Murphy et al., 2004a) and they may have been situated sufficiently close to the Proto-Andean margin to act as a source for Neoproterozoic detritus. Ganderia probably has the most similar Proterozoic–Cambrian tectonic evolution as the Proto-Andean margin (van Staal et al., 1996). It is possible that this peri-Gondwanan terrane was attached to the northwest Amazonian craton during the late Neoproterozoic (see Fig. 10A in van Staal et al., 1996).

6. Summary

We provide examples of detrital zircon populations from autochthonous rocks from the northern and central segments of the Proto-Andean margin of South America, which formed part of the western margin of Gondwana during the Late Neoproterozoic–Palaeozoic. The Proto-Andean margin can be demonstrated to be the source region for most samples. In particular, prominent detrital age peaks between 450 Ma and 500 Ma and 900–1300 Ma have obvious local sources in an Early Ordovician magmatic belt in the Eastern Cordillera of Peru (Chew et al., 2007a) and both the Sunsas orogen of the Southwest Amazonian craton and contiguous basement domains of similar (Grenvillian) age that are discontinuously exposed along the northern Andes (Cordani et al., 2005). However, a significant population in the detrital zircon record (in the 500–650 Ma age range) is ubiquitous in samples from the Proto-Andean margin from Ecuador to Southern Argentina. In the northern and central Andes there is no obvious source for this detritus, and we suggest that a magmatic belt of this age is buried underneath the present-day Andean foreland basin. As there is a marked reduction in the amount of Late Neoproterozoic detritus from the Eocene to the Oligocene in the foreland basin of the north-central Andes (Martin-Gombojav and Winkler, 2008), and this overlaps with the main phase of crustal shortening in the northern Central Andes, we suggest that the Late Neoproterozoic magmatic belt was buried during the Eocene–Oligocene.

Recent studies have demonstrated that the dominantly A-type felsic magmatism within the southern Appalachians (760–680 Ma) (Aleinikoff et al., 1995; Tollo et al., 2004) now has temporal counterparts (775–690 Ma) on the Proto-Andean margin (Baldo et al., 2006; Miškovic et al., in press, Fig. 2). Separation and formation of a Proto-Iapetan ocean (of uncertain width) is inferred in the vicinity of the southern Appalachians at 700 Ma. Subsequent consumption of this oceanic lithosphere on the Proto-Andean side of the ocean, possibly related to the approach of peri-Gondwanan terranes, resulted in the formation of an active margin at around 650 Ma. A Neoproterozoic start to subduction along the South American margin of western Gondwana would therefore be very similar in timing to its inception on the eastern margin of Gondwana (Cawood, 2005; Cawood and Buchan, 2007). The initiation of subduction in east and west Gondwana would therefore temporally correspond with initial assembly and collision of Gondwana blocks.

Acknowledgements

This study was part-funded by a Swiss National Science Foundation grant awarded to Urs Schaltegger. We are extremely grateful to J. Macharé, R. Mucho, A. Sanchez, J. Galdos, A. Zapata, S. Carrasco and R. Mamani of the Geological Survey of Peru (INGEMMET) and C. Moreno of San Marcos University in Lima and for scientific and logistical support during field seasons in Peru. The financial and logistical support of L. Seijas and S.A. Compania Minera Poderosa is also gratefully acknowledged. This is Nordsim publication 215. The Nordsim facility is financed and operated under an agreement between the research councils of Denmark, Norway and Sweden, the Geological Survey of Finland and the Swedish Museum of Natural History. Alex Ulianov is acknowledged for maintenance of the LA-ICPMS facility at the University of Lausanne. The careful and insightful reviews of Victor Ramos and Cees van Staal and the comments of editor Peter Cawood have benefited this article and are gratefully acknowledged.

Appendix A. Analytical technique

Zircons were separated from several kilograms of sample by conventional means. The sub-300 μm fraction was processed using a Wilfey table, and then the Wilfey heavies were passed through a Frantz magnetic separator at 1 A. The non-paramagnetic portion was then settled through di iodomethane. The resulting heavy fraction was then passed again through the Frantz magnetic separator at full current and a side slope of 10°. All zircons were hand picked in ethanol using a binocular microscope, including those for detrital zircon analysis.

For LA-ICPMS analyses, zircon grains were mounted into epoxy resin blocks and polished to obtain flat surfaces. This was followed by cathodoluminescence imaging of individual zircon grains with an SEM microscope to image the internal structures of grains. Samples were analyzed using a 193-nm Excimer laser ablation attached to a PerkinElmer 6100 ICPMS at the University of Lausanne. We applied both rastering and spot mode of data collection depending on the grain size. Rastering acquisition consisted of 1400 readings, comprising 350 blank readings and 1050 data readings, whereas

spot analyses comprised 200 blank readings and 500 data readings. Output laser energy varied between 120 and 160 mJ/pulse for a 30-μm beam diameter. A repetition rate of 10 Hz and 4 Hz was used for rastering and spot analyses, respectively. Helium was used as a carrier gas (1.1 L min^{-1}) for the ablated material from the ablation cell. External correction of laser-induced Pb/U fractionation was monitored by repeated measurements of two reference zircons with known ages, Plesovice (336.45 Ma ± 0.13 Ma, Slama et al., 2008) and 91500 (1065.4 ± 0.3 Ma, Wiedenbeck et al., 1995). For internal correction of mass bias during analysis, Tl–U tracer solution (natural Tl mixed with artificial ^{233}U–^{236}U; $^{236}U/^{233}U = 0.8450$ and $^{205}Tl/^{233}U = 1.2$) was aspirated through Apex desolvating nebuliser and mixed online with the sample aerosol before reaching the plasma (Horn et al., 2000; Košler et al., 2002). Data were processed through in-house Excel macros (LAMDATE, J. Košler). Rastering typically yielded a two-fold improvement in precision over spot analysis. During the course of this study, the Plesovice zircon yielded an age of 336.8 ± 1.4 Ma (2σ; $n = 143$), which is identical, within error, to the reported value of 336.45 ± 0.13 Ma (Slama et al., 2008). The well-characterized 91500 zircon standard gave an age of 1064.1 ± 7.5 Ma (2σ; $n = 49$) which is also in agreement with its accepted age (Wiedenbeck et al., 1995).

For ion microprobe analyses, zircons were mounted in a resin disk along with the zircon standard (91,500) and polished to reveal the grain interiors. The mounts were gold-coated and imaged with a Hitachi S-4300 scanning electron microscope (SEM), using a cathodoluminescence probe (CL) to image internal structures, overgrowths and zonation. Secondary electron mode (SE) imaging was employed to detect fractures and inclusions within the grains. U–Th–Pb zircon analyses (Table 1) were performed on a Cameca IMS 1270 ion-microprobe following methods described by Whitehouse and Kamber (2005) as modified from Whitehouse et al. (1999). U/Pb ratio calibration was based on repeat analyses of the Geostandards zircon 91500, which has an age of 1065.4 ± 0.3 Ma and U and Pb concentrations of 80 ppm and 15 ppm, respectively (Wiedenbeck et al., 1995). Data reduction employed Excel macros developed by Whitehouse at the Swedish Natural History Museum, Stockholm. Age calculations were made using Isoplot version 3.02 (Ludwig, 2003). U–Pb data are plotted as 2σ error ellipses (Fig. 4b). All age errors quoted in the text are 2σ unless specifically stated otherwise. Common lead corrections were only applied only to ion-microprobe results, which exhibited significant levels of ^{204}Pb, and are indicated in Table 1. Common Pb correction uses a modern-day average terrestrial common Pb composition (Stacey and Kramers, 1975; $^{207}Pb/^{206}Pb = 0.83$) assuming that in the high spatial resolution micro-analysis common Pb will enter solely from surface contamination in cracks, as inclusions were avoided. The modern-day Pb composition of Stacey and Kramers (1975) has been demonstrated as appropriate for the Nordsim Laboratory (Kirkland et al., 2008; $^{207}Pb/^{206}Pb = 0.834$).

Appendix B. Supplementary data

Supplementary data associated with this article can be found, in the online version, at doi:10.1016/j.precamres.2008.08.002.

References

Adams, C.J., Miller, H., Toselli, A.J., 2007. Detrital zircon ages of the Puncoviscana Formation of NW Argentina, and their bearing on stratigraphic age and provenance. In: 20th Colloquium on Latin American Earth Sciences, Kiel, pp. 68–69.

Aleinikoff, J.N., Zartman, R.E., Walter, M., Rankin, D.W., Lyttle, P.T., Burton, W.C., 1995. U–Pb ages of metarhyolites of the Catoctin and Mount Rogers formations. Central and Southern Appalachians: evidence for two pulses of Iapetan rifting. American Journal of Science 295 (4), 428–454.

Augustsson, C., Munker, C., Bahlburg, H., Fanning, C.M., 2006. Provenance of late Palaeozoic metasediments of the SW South American Gondwana margin: a combined U–Pb and Hf-isotope study of single detrital zircons. Journal of the Geological Society, London 163 (6), 983–995.

Bachmann, G., Grauert, B., Kramm, U., Lork, A., Miller, H., 1987. El magmatismo del Cámbrico Medio-Cámbrico Superior en el basamento del Noroeste Argentina: investigaciones isotópicas y geocronológicas sobre los granitoides de los complejos intrusivos de Santa Rosa de Tastil y Cañañí. X Congresso Geológico Argentino Actas 4, 125–127.

Bahlburg, H., Vervoort, J.D., 2007. LA-ICP-MS geochronology of detrital zircons in Late Paleozoic turbidte units of northern Chile: implications for terrane processes. Geochimica et Cosmochimica Acta 71 (15S), A51.

Baldo, E., Casquet, C., Pankhurst, R.J., Galindo, C., Rapela, C.W., Fanning, C.M., Dahlquist, J., Murra, J., 2006. Neoproterozoic A-type magmatism in the Western Sierras Pampeanas (Argentina): evidence for Rodinia break-up along a proto-Iapetus rift? Terra Nova 18 (6), 388–394.

Bingen, B., Demaiffe, D., van Breemen, O., 1998. The 616 Ma Old Egersund Basaltic Dyke Swarm, SW Norway, and Late Neoproterozoic opening of the Iapetus Ocean. Journal of Geology 106, 565–574.

Bond, G.C., Nickeson, P.A., Kominz, M.A., 1984. Break up of a supercontinent between 625 Ma and 555 Ma: new evidence and implications for continental histories. Earth and Planetary Science Letters 70 (2), 325–345.

Burkley, L.A., 1976. Geochronology of the Central Venezuelan Andes. Case Western Reserve University, 150 pp.

Caldas, J., 1979. Evidencias de una glaciación Precambriana en la costa sur del Perú, Segundo Congreso Geológico Chileno, Arica, 29–37.

Cardona, A., Cordani, U., Ruiz, J., Valencia, V., Nutman, A., Sánchez, A., 2006. U/Pb detrital zircon geochronology and Nd isotopes from Paleozoic metasedimentary rocks of the Marañon Complex: insights on the proto-Andean tectonic evolution of the Eastern Peruvian Andes. In: Fifth South American Symposium on Isotope Geology, Punta del Este, Uruguay, April 24–25, pp. 208–211.

Cardona, A., Cordani, U.G., Sanchez, A., 2007. Metamorphic, geochronological and geochemical constraints from the Pre-Permian basement of the eastern Peruvian Andes (10° S): a Paleozoic extensional-accretionary orogen? In: 20th Colloquium on Latin American Earth Sciences, Kiel, Germany, pp. 29–30.

Carrascal-Miranda, E.R., Suárez-Ruiz, I., 2004. Short description of the Peruvian coal basins. International Journal of Coal Geology 58 (1/2), 107–117.

Carter, B.T., Hibbard, J.P., Tubrett, M., Sylvester, P., 2006. Detrital zircon geochronology of the Smith River Allochthon and Lynchburg Group, southern Appalachians: implications for Neoproterozoic–Early Cambrian paleogeography. Precambrian Research 147 (3/4), 279–304.

Casquet, C., Pankhurst, R.J., Galindo, C., Rapela, C., Fanning, C.M., Baldo, E., Dahlquist, J., González Casado, J.M., Colombo, F., in press. A deformed alkaline igneous rock–carbonatite complex from the Western Sierras Pampeanas, Argentina: evidence for late Neoproterozoic opening of the Clymene Ocean? Precambrian Research, doi:10.1016/j.precamres.2008.06.011.

Cawood, P.A., 2005. Terra Australis Orogen: Rodinia breakup and development of the Pacific and Iapetus margins of Gondwana during the Neoproterozoic and Paleozoic. Earth Science Reviews 69 (3/4), 249–279.

Cawood, P.A., Buchan, C., 2007. Linking accretionary orogenesis with supercontinent assembly. Earth Science Reviews 82, 217–256.

Cawood, P.A., McCausland, P.J.A., Dunning, G.R., 2001. Opening Iapetus: constraints from the Laurentian margin in Newfoundland. Geological Society of America Bulletin 113 (4), 443–453.

Cawood, P.A., Nemchin, A.A., Strachan, R., 2007. Provenance record of Laurentian passive-margin strata in the northern Caledonides: Implications for paleodrainage and paleogeography. Bulletin of the Geological Society of America 119 (7/8), 993.

Chew, D.M., Kirkland, C.L., Schaltegger, U., Goodhue, R., 2007b. Neoproterozoic glaciation in the Proto-Andes: tectonic implications and global correlation. Geology 35 (12), 1095–1099.

Chew, D.M., Schaltegger, U., Košler, J., Whitehouse, M.J., Gutjahr, M., Spikings, R.A., Miškovic, A., 2007a. U–Pb geochronologic evidence for the evolution of the Gondwanan margin of the north-central Andes. Geological Society of America Bulletin 119 (5/6), 697–711.

Collins, A., Buchan, C., 2004. Provenance and age constraints of the South Stack Group, Anglesey, UK: U–Pb SIMS detrital zircon data. Journal of the Geological Society, London 161 (5), 743–746.

Cordani, U.G., Cardona, A., Jimenez, D.M., Liu, D., Nutman, A.P., 2005. Geochronology of Proterozoic basement inliers in the Colombian Andes: tectonic history of remnants of a fragmented Grenville belt. In: Vaughan, A.P.M., Leat, P.T., Pankhurst, R.J. (Eds.), Terrane Processes at the Margins of Gondwana. Geological Society London Special Publications, pp. 329–346.

Cordani, U.G., Sato, K., Teixeira, W., Tassinari, C.C.G., Basei, M.A.S., 2000. Crustal evolution of the South American platform. In: Cordani, U.G., Milani, E.J., Thomaz Filho, A., Campos, D.A. (Eds.), Tectonic evolution of South America. 31st International Geological Congress. Rio de Janeiro, pp. 19–40.

D'Agrella-Filho, M.S., Tohver, E., Santos, J.O.S., Elming, S.-Å., Trindade, R.I.F., Pacca, I.I.G., Geraldes, M.C., 2008. Direct dating of paleomagnetic results from Precambrian sediments in the Amazon craton: evidence for Grenvillian emplacement of exotic crust in SE Appalachians of North America. Earth and Planetary Science Letters 267 (1/2), 188–199.

Dalmayrac, B., Laubacher, G., Marocco, R., 1980. Géologie des Andes péruviennes: caractères généraux de l'évolution géologique des Andes péruviennes, vol. 122. Travaux et Document de l'ORSTROM, Paris, 501 pp.

Dalziel, I.W.D., 1994. Precambrian Scotland as a Laurentia-Gondwana Link—origin and significance of Cratonic Promontories. Geology 22 (7), 589–592.

de Almeida, F.F.M., de Brito Neves, B.B., Dal Ré Carneiro, C., 2000. The origin and evolution of the South American Platform. Earth Science Reviews 50 (1/2), 77–111.
de Brito Neves, B.B., Neto, C.M.C., Fuck, R.A., 1999. From Rodinia to Western Gondwana: an approach to the Brasiliano-Pan African cycle and orogenic collage. Episodes 22 (3), 155–166.
Dewey, J., Mange, M., 1999. Petrography of Ordovician and Silurian sediments in the western Ireland Caledonides: tracers of a short-lived Ordovician continent-arc collision orogeny and the evolution of the Laurentian Appalachian-Caledonian margin. In: MacNiocaill, C., Ryan, P.D. (Eds.), Continental Tectonics. Geological Society of London, Special Publications, pp. 55–107.
Escayola, M.P., Pimentel, M.M., Armstrong, R., 2007. Neoproterozoic backarc basin: Sensitive high-resolution ion microprobe U–Pb and Sm–Nd isotopic evidence from the Eastern Pampean Ranges, Argentina. Geology 35 (6), 495–498.
Gradstein, F.M., Ogg, J.G., Smith, A.G., 2004. A Geologic Time Scale 2004. Cambridge University Press, 589 pp.
Gutiérrez-Alonso, G., Fernández-Suárez, J., Jeffries, T.E., Jenner, G.A., Tubrett, M.N., Cox, R., Jackson, S.E., 2003. Terrane accretion and dispersal in the northern Gondwana margin. An Early Paleozoic analogue of a long-lived active margin. Tectonophysics 365 (1–4), 221–232.
Hervé, F., Fanning, C.M., Pankhurst, R.J., 2003. Detrital zircon age patterns and provenance of the metamorphic complexes of southern Chile. Journal of South American Earth Sciences 16 (1), 107–123.
Hoffman, P.F., 1991. Did the breakout of Laurentia turn Gondwanaland inside-out? Science 252 (5011), 1409–1412.
Horn, I., Rudnick, R.L., McDonough, W.F., 2000. Precise elemental and isotope ratio determination by simultaneous solution nebulization and laser ablation-ICP-MS: application to U–Pb geochronology. Chemical Geology 164 (3), 281–301.
Hoskin, P.W.O., Schaltegger, U., 2003. The composition of Zircon and igneous and metamorphic petrogenesis. In: Hanchar, J.M., Hoskin, P.W.O. (Eds.), Reviews in Mineralogy and Geochemistry. Mineralogical Society of America, pp. 27–62.
Ingle, S., Mueller, P.A., Heatherington, A.L., Kozuch, M., 2003. Isotopic evidence for the magmatic and tectonic histories of the Carolina terrane: implications for stratigraphy and terrane affiliation. Tectonophysics 371 (1–4), 187–211.
Kamo, S.L., Gower, C.F., Krogh, T.E., 1989. Birthdate for the Iapetus Ocean? A precise U–Pb zircon and baddelyite age for the Long Range dikes, southeast Labrador. Geology 17 (7), 602–605.
Keppie, J.D., Bahlburg, H., 1999. Puncoviscana formation of northwestern and central Argentina: passive margin or foreland basin deposit. In: Ramos, V.A., Keppie, J.D. (Eds.), Laurentia–Gondwana Connections Before Pangea, vol. 336. Geological Society of America, Special Paper, pp. 139–143.
Keppie, J.D., Davis, D.W., Krogh, T.E., 1998. U–Pb geochronological constraints on Precambrian stratified units in the Avalon composite Terrane of Nova Scotia, Canada: tectonic implications. Canadian Journal of Earth Sciences 35, 222–236.
Kinny, P.D., Strachan, R.A., Kocks, H., Friend, C.R.L., 2003. U–Pb geochronology of late Neoproterozoic augen granites in the Moine Supergroup, NW Scotland: dating of rift-related, felsic magmatism during supercontinent break-up? Journal of the Geological Society, London 160 (6), 925–934.
Kirkland, C.L., Daly, J.S., Whitehouse, M.J., 2008. Basement-cover relationships of the Kalak Nappe Complex, Arctic Norwegian Caledonides and constraints on Neoproterozoic terrane assembly in the North Atlantic region. Precambrian Research 160 (3/4), 245–276.
Košler, J., Fonneland, H., Sylvester, P., Tubrett, M., Pedersen, R.B., 2002. U–Pb dating of detrital zircons for sediment provenance studies—a comparison of laser ablation ICPMS and SIMS techniques. Chemical Geology 182 (2–4), 605–618.
Leon, W., Palacios, O., Vargas, L., Sanchez, A., 2000. Memoria explicativa del Mapa Geologico del Peru (1999), Carta Geológica Nacional, Boletín No. 136, escala 1:1,000,000. Instituto Geológico Minero y Metalúrgico, Lima.
Li, Z.X., Bogdanova, S.V., Collins, A.S., Davidson, A., De Waele, B., Ernst, R.E., Fitzsimons, I.C.W., Fuck, R.A., Gladkochub, D.P., Jacobs, J., Karlstrom, K.E., Lu, S., Natapov, L.M., Pease, V., Pisarevsky, S.A., Thrane, K., Vernikovsky, V., 2008. Assembly, configuration, and break-up history of Rodinia: a synthesis. Precambrian Research 160, 179–210.
Litherland, M., Aspden, J.A., Jemielita, R.A., 1994. The Metamorphic Belts of Ecuador, vol. 11. Overseas Memoir of the British Geological Survey, 147 pp.
Loewy, S.L., Connelly, J.N., Dalziel, I.W.D., 2004. An orphaned basement block: the Arequipa–Antofalla basement of the central Andean margin of South America. Geological Society of America Bulletin 116 (1/2), 171–187.
Ludwig, K.R., 2003. User's Manual for Isoplot 3.00: A Geochronological Toolkit for Microsoft Excel, vol. 4. Berkeley Geochronology Center Special Publication, pp. 1–70.
Marechal, P., 1983. Les témoins de la chaîne hercynienne dans le noyau ancien des Andes de Mérida (Venezuela): structure et évolution tectonométamorphique. Université de Bretagne Occidentale, Brest, 176 pp.
Martignole, J., Martelat, J.E., 2003. Regional-scale Grenvillian-age UHT metamorphism in the Mollendo–Camana block (basement of the Peruvian Andes). Journal of Metamorphic Geology 21 (1), 99–120.
Martin-Gombojav, N., Winkler, W., 2008. Recycling of Proterozoic crust in the Andean Amazon foreland of Ecuador—implications for orogenic development of the Northern Andes. Terra Nova.
McCausland, P.J.A., Van der Voo, R., Hall, C.M., 2007. Circum–Iapetus paleogeography of the Precambrian–Cambrian transition with a new paleomagnetic constraint from Laurentia. Precambrian Research 156 (3/4), 125–152.
Miškovic, A., Schaltegger, U., Spikings, R.A., Chew, D.M., Košler, J., in press. Tectonomagmatic evolution of Western Amazonia: geochemical characterization and zircon U–Pb geochronologic constraints from the Peruvian Eastern Cordillera granitoids. Geological Society of America Bulletin.
Murphy, J.B., Fernández-Suárez, J., Jeffries, T.E., Strachan, R.A., 2004b. U–Pb (LA-ICP-MS) dating of detrital zircons from Cambrian clastic rocks in Avalonia: erosion of a Neoproterozoic arc along the northern Gondwanan margin. Journal of the Geological Society, London 161 (2), 243–254.
Murphy, J.B., Pisarevsky, S.A., Nance, R.D., Keppie, J.D., 2004a. Neoproterozoic–Early Paleozoic evolution of peri-Gondwanan terranes: implications for Laurentia–Gondwana connections. International Journal of Earth Sciences 93 (5), 659–682.
Murphy, J.B., Strachan, R.A., Nance, R.D., Parker, K.D., Fowler, M.B., 2000. Proto-Avalonia: a 1.2–1.0 Ga tectonothermal event and constraints for the evolution of Rodinia. Geology 28 (12), 1071–1074.
Omarini, R.H., Sureda, R.J., Götze, H.J., Seilacher, A., Pflüger, F., 1999. Puncoviscana folded belt in northwestern Argentina: testimony of Late Proterozoic Rodinia fragmentation and pre-Gondwana collisional episodes. International Journal of Earth Sciences 88 (1), 76–97.
Pankhurst, R.J., Rapela, C.W., Fanning, C.M., Marquez, M., 2006. Gondwanide continental collision and the origin of Patagonia. Earth-Science Reviews 76 (3/4), 235–257.
Pankhurst, R.J., Rapela, C.W., Saavedra, J., Baldo, E., Dahlquist, J., Pascua, I., Fanning, C.M., 1998. The Famatinian magmatic arc in the central Sierras Pampeanas: an Early to Mid-Ordovician continental arc on the Gondwana margin. In: Pankhurst, R.J., Rapela, C.W. (Eds.), The Proto-Andean Margin of Gondwana, vol. 142. Geological Society London Special Publications, pp. 343–367.
Pimentel, M.M., Fuck, R.A., Botelho, N.F., 1999. Granites and the geodynamic history of the neoproterozoic Brasília belt, Central Brazil: a review. Lithos 46 (3), 463–483.
Polliand, M., Schaltegger, U., Frank, M., Fontboté, L., 2005. Formation of intra-arc volcanosedimentary basins in the western flank of the central Peruvian Andes during Late Cretaceous oblique subduction: field evidence and constraints from U–Pb ages and Hf isotopes. International Journal of Earth Sciences 94 (2), 231–242.
Pratt, W.T., Duque, P., Ponce, M., 2005. An autochthonous geological model for the eastern Andes of Ecuador. Tectonophysics 399 (1–4), 251–278.
Ramos, V.A., 1988. Late Proterozoic–Early Paleozoic of South-America—a collisional history. Episodes 11 (3), 168–174.
Ramos, V.A., 2004. Cuyania, an Exotic Block to Gondwana: Review of a Historical Success and the Present Problems. Gondwana Research 7 (4), 1009–1026.
Ramos, V.A., 2008. The basement of the Central Andes: the Arequipa and related terranes. Annual Review of Earth and Planetary Sciences, 36.
Ramos, V.A., Aleman, A., 2000. Tectonic evolution of the Andes. In: Cordani, U.G., Milani, E.J., Thomaz Filho, A., Campos, D.A. (Eds.), Tectonic Evolution of South America. 31st International Geological Congress. Rio de Janeiro, pp. 635–685.
Ramos, V.A., Jordan, T.E., Allmendinger, R.W., Mpodozic, C., Kay, S.M., Cortés, J.M., Palma, M.A., 1986. Paleozoic terranes of the central Argentine–Chilean Andes. Tectonics 5, 855–880.
Rapela, C.W., Pankhurst, R.J., Casquet, C., Baldo, E., Saavedra, J., Galindo, C., 1998. Early evolution of the Proto-Andean margin of South America. Geology 26 (8), 707–710.
Rapela, C.W., Pankhurst, R.J., Casquet, C., Fanning, C.M., Baldo, E.G., González-Casado, J.M., Galindo, C., Dahlquist, J., 2007. The Río de la Plata craton and the assembly of SW Gondwana. Earth-Science Reviews 83 (1/2), 49–82.
Restrepo-Pace, P.A., Ruiz, J., Gehrels, G., Cosca, M., 1997. Geochronology and Nd isotopic data of Grenville-age rocks in the Colombian Andes: new constraints for late Proterozoic Early Paleozoic paleocontinental reconstructions of the Americas. Earth and Planetary Science Letters 150 (3/4), 427–441.
Reusch, D.N., Van Staal, C.S., McNicoll, V.J., 2004. Detrital zircons and Ganderia's southern margin, Coastal Maine, Geological Society of America Abstracts with Programs, Southeastern Section (53rd Annual) Joint Meeting, p. 129.
Rogers, N., van Staal, C.R., McNicoll, V., Pollock, J., Zagorevski, A., Whalen, J., 2006. Neoproterozoic and Cambrian arc magmatism along the eastern margin of the Victoria Lake Supergroup: a remnant of Ganderian basement in central Newfoundland? Precambrian Research 147 (3/4), 320–341.
Sadowski, G.R., Bettencourt, J.S., 1996. Mesoproterozoic tectonic correlations between eastern Laurentia and the western border of the Amazon Craton. Precambrian Research 76 (3), 213–227.
Slama, J., Košler, J., Condon, D.J., Crowley, J.L., Gerdes, A., Hanchar, J.M., Horstwood, S.A.M., Morris, G.A., Nasdala, L., Norberg, N., Schaltegger, U., Schoene, B., Tubrett, M.N., Whitehouse, M.J., 2008. Plešovice zircon—a new natural reference material for U–Pb and Hf isotopic microanalysis. Chemical Geology.
Stacey, J.S., Kramers, J.D., 1975. Approximation of terrestrial lead isotope evolution by a two-stage model. Earth and Planetary Science Letters 26 (2), 207–221.
Steenken, A., Siegesmund, S., Lopez de Luchi, M.G., Frei, R., Wemmer, K., 2006. Neoproterozoic to Early Palaeozoic events in the Sierra de San Luis: implications for the Famatinian geodynamics in the Eastern Sierras Pampeanas (Argentina). 163 (6), 965–982.
Steiger, R.H., Jäger, E., 1977. Subcommission on geochronology: Convention on the use of decay constants in geo- and cosmochronology. Earth and Planetary Science Letters 36 (3), 359–362.
Tassinari, C.C.G., Macambira, M.J.B., 1999. Geochronological provinces of the Amazonian Craton. Episodes 22 (3), 174–182.
Thomas, W.A., Astini, R.A., Mueller, P.A., Gehrels, G.E., Wooden, J.L., 2004. Transfer of the Argentine Precordillera terrane from Laurentia: constraints from detrital-zircon geochronology. Geology 32 (11), 965–968.

Tohver, E., Bettencourt, J.S., Tosdal, R., Mezger, K., Leite, W.B., Payolla, B.L., 2004. Terrane transfer during the Grenville orogeny: tracing the Amazonian ancestry of southern Appalachian basement through Pb and Nd isotopes. Earth and Planetary Science Letters 228 (1/2), 161–176.

Tohver, E., van der Pluijm, B.A., Van der Voo, R., Rizzotto, G., Scandolara, J.E., 2002. Paleogeography of the Amazon craton at 1.2 Ga: early Grenvillian collision with the Llano segment of Laurentia. Earth and Planetary Science Letters 199 (1/2), 185–200.

Tollo, R.P., Aleinikoff, J.N., Bartholomew, M.J., Rankin, D.W., 2004. Neoproterozoic A-type granitoids of the central and southern Appalachians: intraplate magmatism associated with episodic rifting of the Rodinian supercontinent. Precambrian Research 128 (1/2), 3–38.

Torsvik, T.H., 2003. The Rodinia Jigsaw Puzzle. Science 300 (5624), 1379–1381.

Trindade, R.I.F., Font, E., D'Agrella-Filho, M.S., Nogueira, A.C.R., Riccomini, C., 2003. Low-latitude and multiple geomagnetic reversals in the Neoproterozoic Puga cap carbonate, Amazon craton. Terra Nova 15 (6), 441–446.

Trompette, R., 1997. Neoproterozoic (~600 Ma) aggregation of Western Gondwana: a tentative scenario. Precambrian Research 82 (1), 101–112.

van Staal, C.R., Sullivan, R.W., Whalen, J.B., 1996. Provenance and tectonic history of the Gander Zone in the Caledonide–Appalachian orogen: implications for the assembly of Avalon. In: Nance, R.D., Thompson, M.D. (Eds.), Avalonian and Related Peri-Gondwanan Terranes of the Circum North Atlantic, vol. 304. Geological Society of America, Special Paper, pp. 347–368.

van Staal, C., Whalen, J., McNicoll, V., Pehrsson, S., Lissenberg, C., Zagorevski, A., van Breemen, O., Jenner, G.A., 2007. The Notre Dame arc and the Taconic orogeny in Newfoundland. In: Hatcher Jr., R.D., Carlson, M.P., McBride, J.H., Martínez Catalán, J.R. (Eds.), 4-D Framework of Continental Crust, vol. 200. Geological Society of America Memoir, pp. 511–552.

Waldron, J.W., van Staal, C.R., 2001. Taconian orogeny and the accretion of the Dashwoods block: A peri-Laurentian microcontinent in the Iapetus Ocean. Geology 29 (9), 811–814.

Weil, A.B., Van der Voo, R., Mac Niocaill, C., Meert, J.G., 1998. The Proterozoic supercontinent Rodinia: paleomagnetically derived reconstructions for 1100–800 Ma. Earth and Planetary Science Letters 154 (1–4), 13–24.

Whitehouse, M.J., Kamber, B.S., 2005. Assigning dates to thin gneissic veins in high-grade metamorphic terranes: a cautionary tale from Akilia, southwest Greenland. Journal of Petrology 46 (2), 291–318.

Whitehouse, M.J., Kamber, B.S., Moorbath, S., 1999. Age significance of U–Th–Pb zircon data from early Archaean rocks of west Greenland—a reassessment based on combined ion-microprobe and imaging studies. Chemical Geology 160 (3), 201–224.

Wiedenbeck, M., Alle, P., Corfu, F., Griffin, W.L., Meier, M., Oberli, F., von Quadt, A., Roddick, J.C., Spiegel, W., 1995. Three natural zircon standards for U–Th–Pb, Lu–Hf, trace element and REE analyses. Geostandards Newsletter 19 (1), 1–23.

Williams, H., Hiscott, R.N., 1987. Definition of the Iapetus rift-drift transition in western Newfoundland. Geology 15 (11), 1044–1047.

Willner, A.P., Gerdes, A., Massonne, H.-J., 2007. Growth of the South American convergent margin (lat. 31°S–36°S) during Late Paleozoic times: a U–Pb and Hf-isotope study of detrital zircons from a fossil accretionary system. Geochimica et Cosmochimica Acta 71 (15S), A1119.

Wilson, J., Reyes, L., Garayar, J. (Eds.), 1995. Geología de los Cuadrángulos de Pallasca, Tayabamba, Corongo, Pomabamba, Carhuaz y Huari, Carta Geológica Nacional Boletín Serie A, v. 60, escala 1:100,000. Instituto Geológico Minero y Metalúrgico, Lima, p. 63.